

**DESIGN AND ANALYSIS OF A REAR WHEEL COVER FOR A CAR USING
COMPUTATIONAL FLUID DYNAMICS (CFD)**

KOGILAN A/L GOVINDASAMY

UNIVERSITI MALAYSIA PAHANG

UNIVERSITI MALAYSIA PAHANG

BORANG PENGESAHAN STATUS TESIS ♦

JUDUL: **DESIGN AND ANALYSIS OF A REAR WHEEL COVER FOR A CAR USING COMPUTATIONAL FLUID DYNAMICS (CFD)**

SESI PENGAJIAN: 2009/2010

Saya KOGILAN A/L GOVINDASAMY (860503-29-5753)
(HURUF BESAR)

mengaku membenarkan tesis (Sarjana Muda/~~Sarjana~~ /~~Doktor Falsafah~~)* ini disimpan di Perpustakaan dengan syarat-syarat kegunaan seperti berikut:

1. Tesis adalah hakmilik Universiti Malaysia Pahang (UMP).
2. Perpustakaan dibenarkan membuat salinan untuk tujuan pengajian sahaja.
3. Perpustakaan dibenarkan membuat salinan tesis ini sebagai bahan pertukaran antara institusi pengajian tinggi.
4. **Sila tandakan (✓)

SULIT

(Mengandungi maklumat yang berdarjah keselamatan atau kepentingan Malaysia seperti yang termaktub di dalam AKTA RAHSIA RASMI 1972)

TERHAD

(Mengandungi maklumat TERHAD yang telah ditentukan oleh organisasi/badan di mana penyelidikan dijalankan)

TIDAK TERHAD

Disahkan oleh:

(TANDATANGAN PENULIS)

(TANDATANGAN PENYELIA)

Alamat Tetap:

**LOT 55J, TAMAN SRI PAUH,
18400 TEMANGAN, BANDAR MACHANG,
KELANTAN DARUL NAIM.**

DEVARAJAN A/L RAMASAMY
(Nama Penyelia)

Tarikh: **17 NOVEMBER 2009**

Tarikh: **17 NOVEMBER 2009**

- CATATAN:
- * Potong yang tidak berkenaan.
 - ** Jika tesis ini SULIT atau TERHAD, sila lampirkan surat daripada pihak berkuasa/organisasi berkenaan dengan menyatakan sekali tempoh tesis ini perlu dikelaskan sebagai atau TERHAD.
 - ♦ Tesis dimaksudkan sebagai tesis bagi Ijazah doktor Falsafah dan Sarjana secara Penyelidikan, atau disertasi bagi pengajian secara kerja kursus dan penyelidikan, atau Laporan Projek Sarjana Muda (PSM).

DESIGN AND ANALYSIS OF A REAR WHEEL COVER FOR A CAR USING
COMPUTATIONAL FLUID DYNAMICS (CFD)

KOGILAN A/L GOVINDASAMY

A report submitted in partial fulfillment of the requirements for the award of the degree
of Bachelor of Mechanical Engineering with Automotive Engineering

Faculty of Mechanical Engineering
Universiti Malaysia Pahang

NOVEMBER 2009

SUPERVISOR DECLARATION

“I hereby declare that I have read this thesis and in my opinion this thesis is sufficient in terms of scope and quality for the award the degree of Bachelor of Mechanical Engineering”

Signature :

Name of Supervisor : DEVARAJAN A/L RAMASAMY

Date : November 2009

STUDENT DECLARATION

I declare that this thesis entitled "Design and analysis of a rear wheel cover for a car using computational Fluid Dynamics (CFD)" is the result of my own research except as cited in the references. The thesis has not been accepted for any degree and is not concurrently submitted in candidature of any other degree.

Signature :

Name : KOGILAN A/L GOVINDASAMY

Date : NOVEMBER 2009

This work is dedicated to my beloved ones,

My Father Mr. Govindasamy Manu

My Mother Mrs. Puspa Sinasamy

My Brother Mr. Sri Tharan Govindasamy

My Sisters Ms. Pannir Selvi Govindasamy and Ms. Sinth Mani Govindasamy

And

My Niece Ms. Sathiavathy Mahendran

ACKNOWLEDGEMENT

I would like to express my deepest appreciation and gratitude to my supervisor, Mr. Devarajan Ramasamy for his guidance, patience for giving advises and supports throughout the progress of this project. Special thanks are also given to all lecturers and vocational trainers for the guidance, experience sharing and comment on my project thesis. They were not hesitant to answer all my doubts and spending their time to guide me during my experimental work.

A great appreciation is acknowledged to the Faculty of Mechanical Engineering for the funding under the final year project.

Last but not least, I would like to thank all my friends for their support and encouragement given to me, especially during the hard times.

ABSTRACT

The performance and handling of automobile are significantly affected by its aerodynamic properties. One of the main causes of aerodynamic is about drag force and lifting force. This will influence all the aspect of the vehicles such as overall performance, fuel consumption, safety and stability. However, the unavoidable need for wheels caused and even recently causes significant problems for aerodynamicists to deal with the flow. The addition of wheelhouses and rotating wheels to an aerodynamically optimized car body, leads to decrease in drag and lift coefficients by 30% and 40%, respectively. In an aerodynamic field, the main important thing to get the stability, performance and good fuel consumption is to design a vehicle with low C_D . The reduction of lift and flow separation is the key results that will be a point of discussion. Rear wheel cover will reduce the flow separation at the wheel houses that causing the turbulent airflow. The wake region also will be reduced and this will make the drag force that produce at the wheel houses will reduced. By the lower drag force will contribute to the lower fuel consumption. The task was done by doing a Computational Fluid Dynamic (CFD) analysis for expected vehicle speed of 40-140 km/h. A drag force was found based on inputs from CFD analysis. This force was calculated to produce the drag coefficient of the model as a whole. The approach needed to justify the amount of drag that can be reduced by addition of a rear wheel cover as compared to the model without the rear wheel cover. This project is to get an overall comparison of the velocity and pressure distribution before and after the rear wheel cover is added. The drag coefficient of the vehicle was decreases from 0.3882 to 0.3773 when adding the rear wheel cover.

ABSTRAK

Ciri-ciri aerodinamik adalah sangat mempengaruhi akan prestasi dan kawalan sesebuah kenderaan. Salah satu kesan penyebab akan aerodinamik adalah geseran atau daya seretan dan daya tujahan. Ini akan mempengaruhi kesemua prestasi, penggunaan minyak, keselamatan, dan kestabilan sesebuah kenderaan. Walaubagaimanapun, penggunaan roda tidak dapat dilelakkan dan ini telah menyebabkan masalah untuk aerodynamis untuk menangani dengan aliran udara. Hasil tambahan penutup tayar dan putaran roda kepada badan kereta yang dioptimumkan secara aerodinamik menyebabkan pekali seret menurun sebanyak 30% dan pekali daya angkat sebanyak 40%. Di dalam aspek aerodinamik, kestabilan, prestasi dan penggunaan minyak amat penting untuk menghasilkan kenderaan yang rendah C_D . Pengurangan tujahan dan peybaran udara adalah kunci utama di dalam perbincangan Penutup tayar belakang juga akan menghasilkan peybaran pengaliran udara yang kurang di belakang kerana ini akan menghasilkan pegaliran udara yang bergelora. Kawasan olak di belakang juga akan berkurangan dan ini akan menjadikan daya geseran yang terhasil di bahagian belakang tayar kenderaan berkurangan. Dengan nilai daya geseran yang rendah, ia akan membantu dalam penggunaan minyak yang rendah. Tugas ini dimulakan dengan menggunakan kelajuan yang telah ditetapkan pada 40 km/j hingga 140 km/j dengan menggunakan analisis Computational Fluid Dynamic (CFD). Daya geseran akan didapati apabila menggunakan perisian maklumat daripada CFD analisis. Nilai daya ini akan digunakan untuk mengira pekali geseran keseluruhan model kereta tersebut. Nilai pengurangan geseran yang terhasil daripada penutup tayar belakang diperlukan untuk membenarkan pembezaan di antara model tanpa penutup tayar di belakang. Projek ini akan mendapatkan perbezaan berdasarkan pegaliran angin dan tekanan sebelum dan selepas penutup tayar belakang dipasangkan. Pekali seret bagi kenderaan menurun dari 0.3882 ke 0.3773 apabila penutup tayar belalang dipasangkan.

TABLE OF CONTENTS

	Page
TITLE	i
SUPERVISOR DECLARATION	ii
STUDENT DECLARATION	iii
DEDICATION	iv
ACKNOWLEDGEMENTS	v
ABSTRACT	vi
ABSTRAK	vii
TABLE OF CONTENTS	viii
LIST OF TABLES	xii
LIST OF FIGURES	xiii
LIST OF SYMBOLS	xvi
LIST OF ABBREVIATION	xvii
LIST OF APPENDICES	xviii
CHAPTER 1 INTRODUCTION	
1.1 Background	1
1.2 Problem Statement	1
1.3 Objectives	2
1.4 Scopes of Study	2

CHAPTER 2 LITERATURE REVIEW

2.1	Automotive Aerodynamics	3
2.2	Aerodynamic Force	4
2.2.1	Forces	4
2.2.2	Aerodynamic Lift	5
2.3	Aerodynamic Pressure	6
2.4	Aerodynamic Drag	8
2.5	Drag Coefficient	9
2.5.1	Drag coefficient and various body shapes	11
2.6	Air Flow around the Vehicle	12
2.6.1	External Flow	13
2.7	Rear Wheel Cover	14
2.7.1	Forces acting on the vehicle	14
2.7.2	Exposed wheel air flow pattern	16
2.7.3	Partial enclosed wheel air flow pattern	18
2.7.4	Sample of Wheel houses	20
2.8	Dynamic Fluid Properties	21
2.8.1	Air Density Properties Related To Vehicle	21
2.8.2	Air Viscosity Properties Related To Vehicle	22
2.9	Friction Drag	22
2.10	Reynolds Number	23
2.11	Fuel Consumption	24
2.12	Result Validation	25

CHAPTER 3 METHODOLOGY

3.1	Introduction	28
-----	--------------	----

3.2	Problem Solving	31
3.2.1	Literature Study	31
3.2.2	Identify Project Objectives	32
3.2.3	Measurement the Rear Wheel Cover	32
3.2.4	Dimension of the HEV Model	33
3.2.5	3-D Car Modeling	33
3.2.6	Sketching Applying For Model Improvement	34
3.2.7	CFD Simulation	35
3.2.8	Mesh Independent Analysis	38

CHAPTER 4 RESULT AND DISCUSSION

4.1	Introduction	41
4.2	Frontal Area of The Model	42
4.3	Drag Coefficient	42
4.4	Aero Power	45
4.5	Percentage Reduction	48
4.5.1	Percentage of Drag Coefficient Reduction	49
4.5.2	Percentage of Aero power Reduction	49
4.6	Simulation Result	49
4.6.1	Simulation of External Pressure Distribution	50
4.6.2	Simulation of External Velocity Distribution	52
4.7	Discussion	55

CHAPTER 5 CONCLUSION AND RECOMMENDATION

5.1	Conclusion	57
5.2	Recommendation	58

REFERENCES	59
APPENDICES	61

LIST OF TABLES

Table No.	Title	Page
2.1	Forces acting on moving vehicle	5
2.2	Typical drag coefficient for various classes of vehicle	9
2.3	Drag and lift coefficients on the surfaces of the basic body (no wheels, no wheelhouses) and the baseline model (wheels and wheelhouses are included)	16
2.4	Experimental and CFD values for drag and lift coefficient of the wheel of Fabijanic's vehicle model with rear wheel cover	26
3.1	Number of cells for each level for the model simulation	40
4.1	Drag coefficient of vehicle with and without rear wheel cover	44
4.2	Aero power of vehicle with and without rear wheel cover	47
4.3	Average values of C_D and P	48

LIST OF FIGURES

Figure No.	Page
2.1 Aerodynamic of bluff bodies	4
2.2 Arbitrary forces and origin of the forces acting on the vehicle	5
2.3 Aerodynamic Lift	6
2.4 Pressure and velocity gradients in the air flow over the body	7
2.5 vortex shedding in flow over a cylindrical body	8
2.6 Drag coefficients of various shapes	10
2.7 Drag coefficients for various shaped soil	12
2.8 Flow around a vehicle	14
2.9 The geometry of the simplified vehicle model of investigation with the Indications of the different surfaces	15
2.10. (a) Wheel rotation in still air away from the ground	17
(b) Air flow pattern with wheel rolling on the Ground	17
(c) Air pressure distribution with wheel rolling on the ground	18
2.11 (a) Wheel arch air flow (Side view)	19
(b) Wheel arch air flow (Plane view)	19
2.12 Affect of underside ground clearance on both lift and drag coefficients	20
2.13 Rear wheel cover for lorry	20
2.14 Rear wheel cover for Pickup Truck	21
2.15 Distribution of velocity and temperature in the vicinity of a wall	22

2.16	Determination of the drag of a body (two-dimensional flow)	23
2.17	Graphic depicting representative horsepower requirements versus vehicle speed for a heavy vehicle tractor-trailer truck	24
2.18	Flow at a stationary wheel and ground:	
	(a) oil-film visualization in wind tunnel	26
	(b) Numerical simulation (wall streak lines)	26
2.19	Comparison of numerical parameter studies with experimental ones	27
3.1	Methodology flow chart for PSM 1	29
3.2	Methodology flow chart for PSM 2	30
3.3	Basic view of the rear Wheel Cover from different side of view	32
3.4	Rear wheel diffuser on the HEV model	33
3.5	(a) Manual drawing from the data sheet (Front View)	34
	(b) 3-Dimensional drawing (Front View)	34
3.6	(a) Manual drawing from the data sheet (Side View)	35
	(b) 3-Dimensional drawing (Side View)	35
3.7	Model view with rear wheel cover	32
3.8	CFD boundary condition with streamlines and Computational Domain size	35
3.9	Simulation of analysis type	36
3.10	(a) Run startup for simulation	37
	(b) Velocity analysis solver for each speed	37
3.12	Mesh Levels analyzed level 2, level 3, level 4 and level 5	38
3.13	Velocity Point for mesh study	39
3.14	Point velocity versus Actual velocity for the model	39
4.1	The frontal area without and with rear wheel cover from the Solid Works	42
4.2	Drag coefficient vs. Speed	44

4.3	Aero power vs. Speed	47
4.4	Comparison of pressure distribution between with and without rear wheel cover	50-51
4.5	Comparison of velocity distribution between with and without rear wheel cover	52-54

LIST OF SYMBOLS

F_L	Lift force
ρ	Density
V	Velocity
V_o	Wind velocity (reversed direction)
A	Area
P	Pressure
P_{atm}	Atmosphere pressure
C_D	Drag coefficient
F_D	Drag force
$^\circ$	Degree of angle
l	Length
P_r	Prevailing pressure
T	Temperature
μ	Viscosity
U	Dynamic viscosity
Re	Reynolds Number
%	Percentage
θ	Angle
P	Aero power

LIST OF ABBREVIATIONS

HEV	Hybrid Electrical Vehicle
CFD	Computational Fluid Dynamic
CAD	Computational Aided Design
km/h	kilometer per hour
m/s	mile per second
mph	mile per hour
mm	millimeter
kW	kilowatt
N	newton

LIST OF APPENDICES

Appendix		Page
A	Gantt Chart For PSM	61
B	Plane Analysis Profile Visualization	63
C	Rear Wheel Cover Model	64
D.	3-D Modeling (Without Rear Wheel Cover)	65
E	3-D Modeling (With Rear Wheel Cover)	66

CHAPTER 1

INTRODUCTION

1.1 Background

A car driven in a road is affected by aerodynamic forces created. In all these categories, the aerodynamics of such cars is of vital importance. They affect the cars stability and handling. They influence both performance and safety. Aerodynamics is the branch of dynamics that deals with the motion of air and other gaseous fluids and with the forces acting on bodies in motion relative to such fluids. For some classes of racing vehicles, it may also be important to produce desirable downwards aerodynamic forces to improve traction and thus cornering abilities. Most everyday things are either caused by aerodynamic effects or in general obey the aerodynamic laws. For aerodynamic bodies a simplified procedure may then be devised for the evaluation of the aerodynamic loads.

1.2 Problem Statement

Most of moving vehicle produces drag because of the turbulent air of airflow separation. These will produce the drag force and the reduction of drag is essential for improving performance and fuel consumption. In the last century, particularly in its last 30 years the possible lowest drag have been approached. In every vehicle movement, the air flow will go through to the wheel houses of the vehicle. This air flow will make the drag and friction. To avoid the air flow through the wheel houses, rear wheel cover is suggested. This device is hoped to reduce the drag force and the drag coefficient when the vehicle moving in high velocity. By this the objectives of the project will achieved.

1.3 Objectives

The objectives of the project are as follows:

- i. To analyze the effect of rear wheel cover on a vehicle in term of drag coefficient.
- ii. To reduce the drag coefficient of the car by modifying the wheel cover area.

1.4 Scopes of Study

The scopes of the project are as follows:

- i. Study on aerodynamics drag reduction by rear wheel cover.
- ii. Redevelop the existing model of rear wheel cover with Solid Works.
- iii. Simulate the model by using Computational Fluid Dynamic (CFD).
- iv. To compare the drag for both with and without rear wheel cover.

CHAPTER 2

LITERATURE REVIEW

2.1 Automotive Aerodynamics

Aerodynamics at cars became more and more important with the increase of their velocity. In the beginning of the 20th century, the shape of vehicles was adopted from the field of aviation and ships. Cars had an aerodynamic shape but their velocity was very low, mainly due to the quality of the roads [14]. Aerodynamics is the branch of dynamics that deals with the motion of air and other gaseous fluids and with the forces acting on bodies in motion relative to such fluids. Automotive aerodynamics is the study of the aerodynamics of road vehicles. The main concerns of automotive aerodynamics are reducing drag, reducing wind noise, minimizing noise emission and preventing undesired lift forces at high speeds. For some classes of racing vehicles, it may also be important to produce desirable downwards aerodynamic forces to improve traction and thus cornering abilities [1]. An aerodynamic automobile will integrate the wheel and lights in its shape to have a small surface. It will be streamlined, for example it does not have sharp edges crossing the wind stream above the windshield and will feature a sort of tail called a fastback or Kammback or lift back. It will have a flat and smooth floor to support the venturi or diffuser effect and produce desirable downwards aerodynamic forces. The air that rams into the engine bay, is used for cooling, combustion, and for passengers, then reaccelerated by a nozzle and then ejected under the floor. Most everyday things are either caused by aerodynamic effects or in general obey the aerodynamic laws. For aerodynamic bodies a simplified procedure may then be devised for the evaluation of the aerodynamic loads.

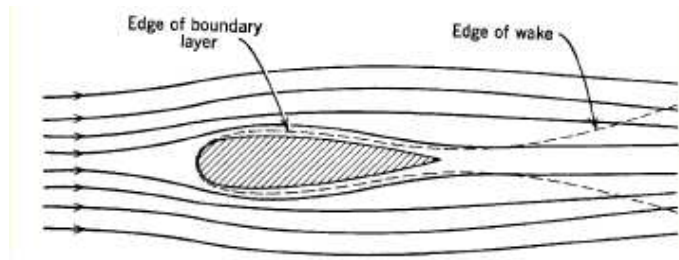


Figure 2.1: Aerodynamic of bluff bodies [1]

A car driven in a road is affected by aerodynamic forces created. The aerodynamics of such cars is of vital importance. They affect the cars stability and handling. They influence both performance and safety.

2.2 Aerodynamic Force

2.2.1 Forces

A body in motion is affected by aerodynamic forces. The aerodynamic force acts externally on the body of a vehicle. The aerodynamic force is the net result of all the changing distributed pressures which airstreams exert on the car surface [3]. Aerodynamic forces interact with the vehicle causing drag, lift, down, lateral forces, moment in roll, pitch and yaw, and noise. These impact fuel economy, and handling. The aerodynamic forces produced on a vehicle arise from two sources that are form (or pressure) drag and viscous friction. Forces and moment are normally defined as they act on the vehicle. Thus a positive force in the longitudinal (x-axis) direction on the vehicle is forward. The force corresponding to the load on a tire acts in the upward direction and is therefore negative in magnitude (in the negative z-direction). The forces also corresponding to the shape on the vehicle part in aerodynamic shape. Figure 2.2 below shown of the vehicle most significant forces [2].

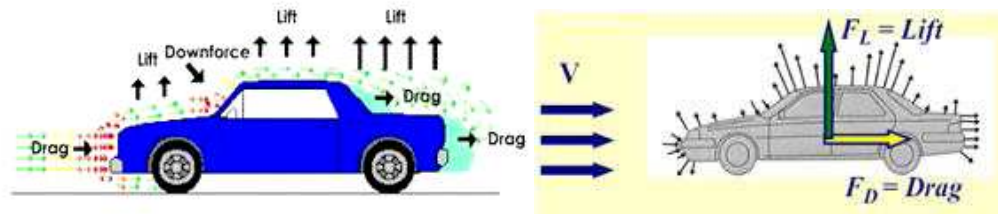


Figure 2.2: Arbitrary forces and origin of the forces acting on the vehicle [2] [3]

Table 2.1: Forces acting on moving vehicle

Direction	Force	Moment
Longitudinal (x -axis, +ve rearward)	Drag	Rolling moment
Lateral (y -axis, +ve to the right)	Side force	Pitching moment
Vertical (z -axis, +ve upward)	Lift	Yawing moment

The focus in cars is on the aerodynamic forces of down force and drag. The relationship between drag and down force is especially important. Aerodynamic improvements in wings are directed at generating down force on the car with a minimum of drag. Down force is necessary for maintaining speed through the corners [3].

2.2.2 Aerodynamic Lift

The other component, directed vertically, is called the aerodynamic lift. It reduces the frictional forces between the tires and the road thus changing dramatically the handling characteristics of the vehicle. In addition to geometry, lift F_L is a function of density ρ and velocity V . Lift is the net force (due to pressure and viscous forces) perpendicular to flow direction. The aerodynamic drag coefficient equation is [2.1].

$$C_F = \frac{F_L}{\frac{1}{2}\rho V^2 A} \quad (2.1)$$

F_L = lift force [N]

ρ = density of the air [kg/m³]

A = area of the body [m²]

V = velocity of the body [m/s]

Aerodynamic lift and its proper front-and-rear-axle distribution is one of the key aspects in terms of on-road stability [4]. As long as driving speed is low, below say 100 km/h, lift and pitching moment have only a small effect on the directional stability of a car, even in crosswind. However, at higher speeds this is no longer true, and so recent developments are directed at controlling them.

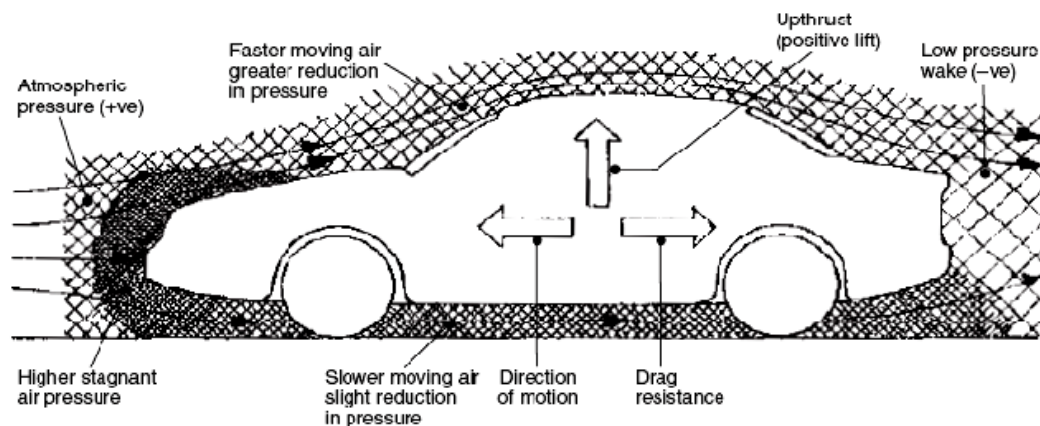


Figure 2.3: Aerodynamic Lift

2.3 Aerodynamic Pressure

The gross flow over the body of a vehicle is governed by the relationship between velocity and pressure expressed in Bernoulli's Equation. Bernoulli's Equation assumes incompressible flow which is reasonable for automotive aerodynamics [2].

$$P_{static} + P_{dynamic} = P_{total} \quad (2.2)$$

$$P_s + \frac{1}{2} \rho V^2 = P_t$$

ρ = density of air [kg/m³]

V = velocity of air (relative to the car) [m/s]

In equation above, the sum of the forces brings in the pressure affect acting on the incremental area of the body of fluid. The static plus the dynamic pressure of the air will be constant (P_t) as it approaches the vehicle. At the distance from the vehicle the static pressure is simply the ambient, or barometric, pressure (P_{atm}). The dynamic pressure is produced by the relative velocity, which is constant for all streamlines approaching the vehicle. As the flow approaches the vehicle, the streamlines split, some going above the vehicle and others below. By inference, one streamline must go straight to the body and stagnate (impinging on the bumper of the vehicle). At that point the relative velocity has gone to the zero. This will make the static pressure observed at that point on the vehicle. Figure 2.4 and Figure 2.5 below showing flow over a cylinder that it affects is most same to the vehicle [2].

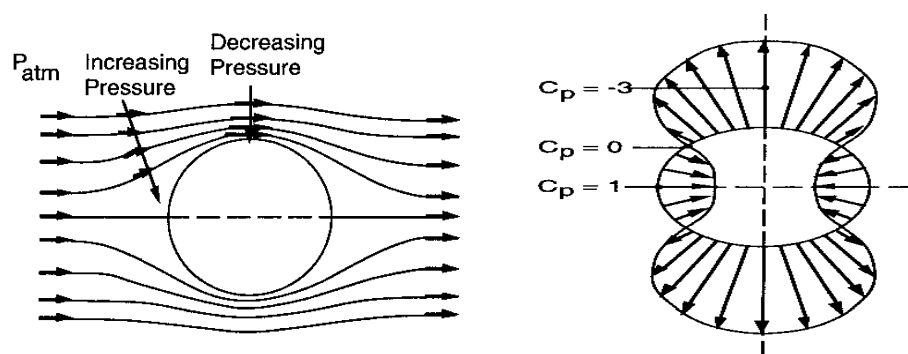


Figure 2.4: Pressure and velocity gradients in the air flow over the body [2]

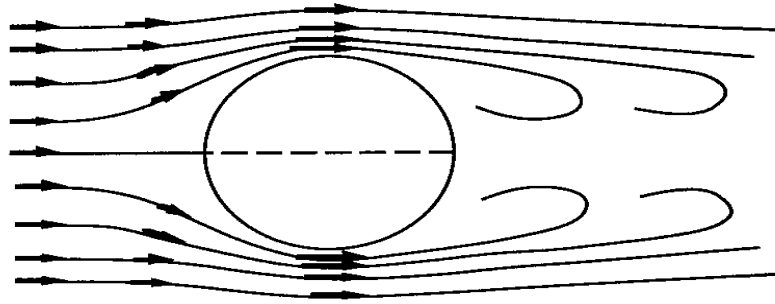


Figure 2.5: Vortex shedding in flow over a cylindrical body [2]

The static pressure will distribute along the body of a car. The pressures are indicated as being negative or positive with to the ambient pressure some distance from the vehicle. A negative pressure is developed at the front edge of the hood as the flow rising over the front of the vehicle attempts to turn and follow horizontally along the hood [2]. Near the base of the windshield and cowl, the flow must be turned upward, thus the high pressure is experienced. Over the roof line the pressure goes negative as the air flow tries to follow the roof contour.

2.4 Aerodynamic Drag

The component of the resultant aerodynamic force which opposes the forward motion is called the aerodynamic drag. The aerodynamic drag affects the performance of a car in both speed and fuel economy as it is the power required to overcome the opposing force. In order to explain the aerodynamic drag, there have two forces that are the frontal pressure and the rear vacuum [5].

Frontal pressure is caused by the air attempting to flow around the front of the car. As millions of air molecules approach the front part of the car, they begin to compress, and in doing so raise the air pressure in front of the car. Rear vacuum or wake is caused by the “hole” left in the air as the car passes through it. This empty area is a result of the air molecules not being able to fill the hole as quickly as the car can make it [5]. The air molecules attempt to fill in to this area, but the car is always one step ahead.

In every moving vehicle, the drag will produce in every surface of the vehicle. The drag is due in part to friction of the air on the surface of the vehicle, and in part to the way the friction alters the main flow down the back side of the vehicle. Drag is the largest and most important aerodynamic force encountered by passenger cars at normal highway speeds. The overall drag on a vehicle derives from contributions of many sources. For the vehicle, the drag produced from the body (for body, after body, under body and skin friction). The major contributor is the after body because of the drag produced by the separation zone at the rear. It is in area that the maximum potential for drag reduction is possible [2].

2.5 Drag Coefficient

The aerodynamic drag coefficient is a measure of the effectiveness of a streamline aerodynamic body shape in reducing the air resistance to the forward motion of a vehicle. A low drag coefficient implies that the streamline shape of the vehicle's body is such as to enable it to move easily through the surrounding viscous air with the minimum of resistance, conversely a high drag coefficient is caused by poor streamlining of the body profile so that there is a high air resistance when the vehicle is in motion. Typical drag coefficient for various classes of vehicle can be seen in Table 2.2 [15].

Table 2.2: Typical drag coefficient for various classes of vehicle [15]

Vehicle type drag coefficient C_D	
Saloon car	0.22-0.40
Sports car	0.28-0.40
Light van	0.35-0.50
Buses and coaches	0.40-0.80
Articulated trucks	0.55-0.80
Ridged truck and draw bar trailer	0.70-0.90

The aerodynamic drag is the focus of public interest in vehicle aerodynamics. It is and even more so it's non-dimensional number of C_D , the drag coefficient has almost become a synonym for the entire discipline. Performance, fuel economy, emissions, and top speed are important attributes of a vehicle because they represent decisive sales arguments, and they all are influenced by drag. Drag coefficient (C_D) is a commonly published rating of a car's aerodynamic smoothness, related to the shape of the car. Multiplying C_D by the car's frontal area gives an index of total drag. The result is called drag area, and is listed below for several cars. The width and height of curvy cars lead to gross overestimation of frontal area. The aerodynamic drag coefficient equation is (2.3)[2]:

$$C_D = \frac{F_D}{\frac{1}{2}\rho V^2 A} \quad (2.3)$$

F_D = drag force [N]

ρ = density of the air [kg/m³]

A = area of the body [m²]

V = velocity of the body [m/s]

The drag coefficient varies over a broad range with different shapes. Figure 2.6 below shows the coefficients for a number of shapes. In each case it is presumed that the air approaching the body has no lateral component. The simple aerofoil has a drag coefficient of 0.007. This coefficient means that the drag force is 0.007 times as large as the dynamic pressure acting over the area of the plate.

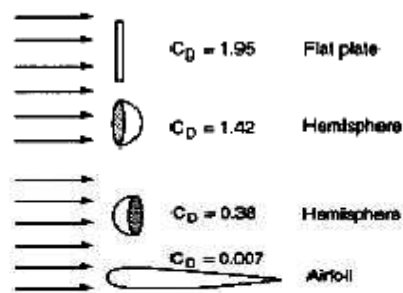


Figure 2.6: Drag coefficients of various shapes [2]

In contrast, with the much better aerodynamic design of cars, their drag coefficient is not as sensitive to yaw angle because the flow will not separate so readily. Normally, the drag coefficient increase by 5% to 10% with yaw angles in the range typical of on-road driving for passenger cars. The different of yaw angle will influence on the drag coefficients of several different types of vehicles [2].

2.5.1 Drag coefficient and various body shapes Figure 2.6 (a-f)

Circular plate as in Figure 2.7(a). Air flow is head on, and there is an immediate end on pressure difference. Flow separation takes place at the rim; this provides a large vortex wake and a correspondingly high drag coefficient of 1.15.

Cube as in Figure 2.7(b). Air flow is head on but a boundary layer around the sides delays the flow separation, nevertheless there is still a large vortex wake and a high drag coefficient of 1.05.

Sixty degree cone as in Figure 2.7(c). With the piecing cone shape air flows towards the cone apex and then spreads outwards parallel to the shape of the cone surface. Flow separation however still takes place at the periphery thereby producing a wide vortex wake. This profile halves the drag coefficient to about 0.5 compared with the circular plate and the cube block.

Sphere as in Figure 2.7(d). Air flow towards the sphere, it is then diverted so that it flows outwards from the centre around the diverging surface and over a small portion of the converging rear half before flow separation occurs. There is therefore a slight reduction in the vortex wake and similarly a marginal decrease in the drag coefficient to 0.47 compared with the 60° cone.

Hemisphere as in Figure 2.7(e). Air flow towards and outwards from the centre of the hemisphere gradually aligns with the main direction of flow after which flow separation takes place on the periphery. For some unknown reason (possibly due to the very gradual alignment of surface curvature with the direction of air movement near the

Rim) the hemisphere provides a lower drag coefficient than the cone and the sphere shapes this, being of the order of 0.42.

Tear drop (Figure 2.7(f)). If the proportion of length to diameter is well chosen, for example 0.25, the streamline shape can maintain a boundary layer before flow separation occurs almost to the end of its tail. Thus the resistance to body movement will be mainly due to viscous air flow and little to do with vortex wake suction with these contours the drag coefficient can be as low as 0.05 [15].

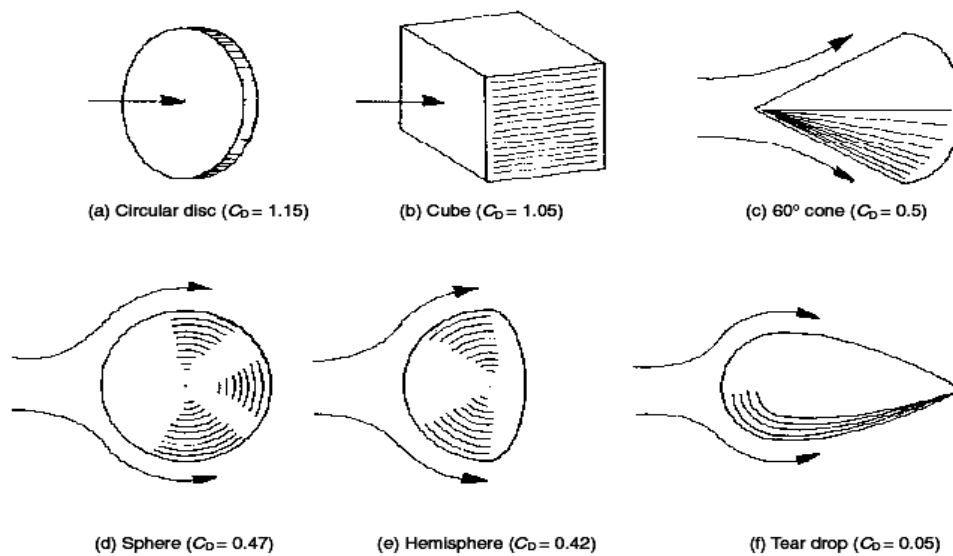


Figure 2.7(a-f): Drag coefficients for various shaped soil [15]

2.6 Air Flow around the Vehicle

Under calm conditions and no traffic, vehicles travel through still air, hence the relative air flow they experience has no turbulence, is unsteadily relative to the vehicle and has the same magnitude as the vehicle speed relative to the road. If an atmospheric wind or air flow is present, generally a yaw angle is created because the flow is not aligned with the centerline of the vehicle and thus the air speed of a vehicle experiences is not the same as the road speed [6].

The flow processes to which a moving vehicle is subjected fall into two categories:

- 1) Flow of air around the vehicle.
- 2) Flow of air through the vehicle's body.

The two categories of these flow fields are closely related. For example, the flow of air through the engine compartment depends on the flow field around the vehicle. Both flow fields must be considered together. On the other hand, the flow processes within the engine and transmission are not directly connected with these two categories of flow. They are not called aerodynamics, and are not treated here [8]. Flow separations may appear in different locations on vehicles with more angular geometries, and fairing dominated flows can exist on a variety of road vehicles. The main aspect of this flow field is the formation of two concentrated side edge vortices which dominate the nearby flow field. Those two vortices induce a large velocity on the plate creating strong suction forces which considerably increase the lift of the flat-plate wing. Typical pattern of flow-separation frequently found on three-box-type sedans. In this case a separated bubble, with locally recirculation flow, is observed in the front, at the break point between the bonnet and the windshield. The large angle created between the rear windshield and trunk area results in a second, similar flow-recirculation area [9] [10].

2.6.1 External Flow

The flow around a vehicle is responsible for its directional stability as well as straight line stability, dynamic passive steering, and response to crosswind depend on the external flow field. Furthermore, the outer flow should be tuned to prevent duplets of rain water from accumulating on windows and outside mirrors, to keep headlights free of dirt, to reduce wind noise, to prevent the windshield wipers from lifting off, and to cool the engine's oil pan, muffler, and brakes, etc. The external flow around a vehicle is shown in Figure 2.8 below. In still air, the undisturbed velocity, V is the road speed of the car. Provided no flow separation takes place, the viscous effects in the fluid are restricted to a thin layer of a few millimeters thickness, called the boundary layer.

Beyond this layer the flow can be regarded as inviscid, and its pressure is imposed on the boundary layer. Within the boundary layer the velocity decreases from the value of the inviscid external flow at the outer edge of the boundary layer to zero at the wall, where the fluid fulfills a no slip condition. When the flow separates, the boundary layer is "dispersed" and the flow is entirely governed by viscous effects. The character of the viscous flow around a body depends only on the body shape and the Reynolds number. For different Reynolds numbers entirely different flows may occur for one and the same body geometry. Thus the Reynolds number is the dimensionless parameter which characterizes a viscous flow [8] [9].

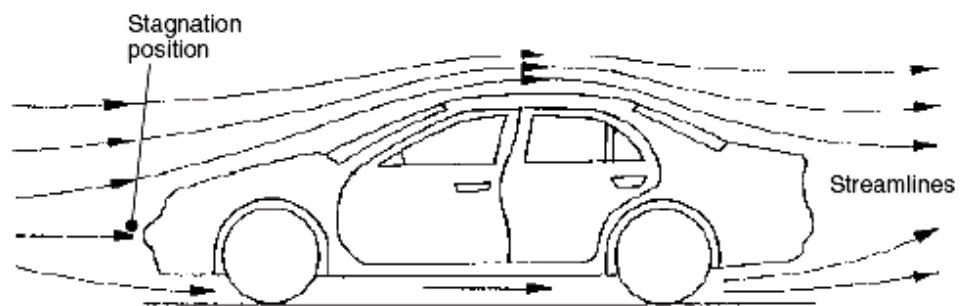


Figure 2.8: Flow around a vehicle [15]

2.7 Rear Wheel Cover

2.7.1 Forces acting on the vehicle

As the model used at the investigation was symmetrical, we were interested in lift and drag only, the side forces were off the present topic. For mapping the origin of forces and to carry out a systematic study, several geometry configurations were tested. First, a baseline model was created that included wheelhouses and rotating wheels according to Figure 2.9. Then the wheelhouse and the wheel were removed to determine the drag and lift acting on the basic body. The effect of the presence of rotating wheel was investigated by including or removing the wheel from the wheelhouse, and finally, the wheelhouse openings were recursively covered in the presence of rotating wheel.

Forces acting on the individual surfaces (shown in Figure 2.9) are reported here in summary. C_D [-] and C_L [-] are the drag and lift coefficients, respectively; F_D [N] and F_L [N] are the drag and lift forces, respectively; V^∞ [m/s] is the free stream velocity and A [m²] is the stream wise total area of the vehicle [16].

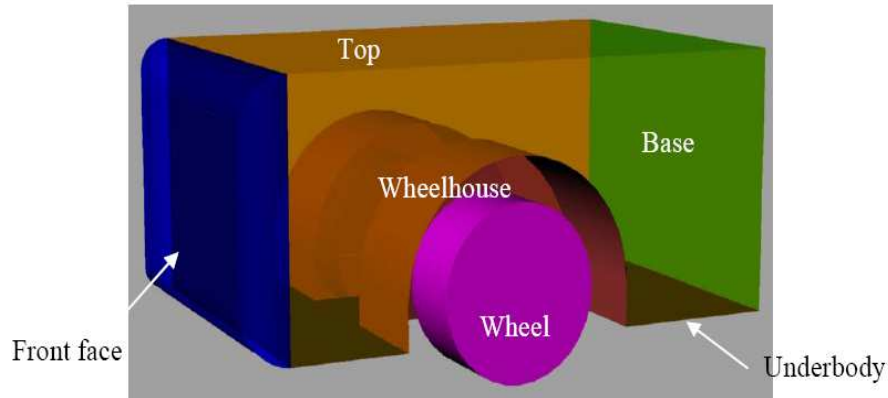


Figure 2.9: The geometry of the simplified vehicle model of investigation with the Indications of the different surfaces [16]

The drag coefficient of the vehicle increases by 62% when wheels and wheelhouses are added to the basic body. Analyzing the components of the drag force one can note that 17% of the increase is originating from the forces acting on the vehicle body due to the modification of the flow field, 9.1% and 35.6% acting on the wheelhouse and the wheel, respectively. One might say that almost 57.4% of the total increase in drag coefficient is the effect of the forces acting on the wheel, while 42.6% of the increase is generated on the body and wheelhouse. However, the wheelhouse contributes in drag only in a very small amount comparing to the wheel.

Lift coefficient changes from 0.0343 to 0.1909 when wheels and wheelhouses were added to the basic body, the lift coefficient of which was, however, very small. The low pressure in the wheelhouse partially cancels the vertical component of forces acting on the wheel and on the wheelhouse and on extending parts of the fender contributes to lift with exerting a down force on the vehicle. The wheel contributes with 0.0998 and the remaining part of the increase in lift is due to the modification of the

flow field and to the pressure increase on the underbody surface of the vehicle in front of the wheels. The wheels block a part of the flow coming in the underbody gap, thus more flow has to move towards the top of the vehicle, generating lower pressure at that region. Thus the pressure on the underbody increases and that on the top of the vehicle decreases, leading to an increase in lift force [15][16].

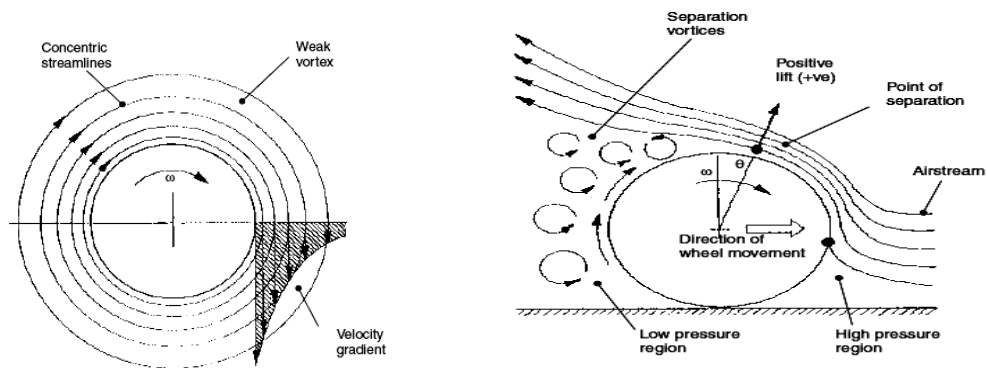
Table 2.3: Drag and lift coefficients on the surfaces of the basic body (no wheels, no Wheelhouses) and the baseline model (wheels and wheelhouses are included) [16]

	Drag coefficient		Lift coefficient	
	Basic body	+wheel+wheelhouse	Basic body	+wheel+wheelhouse
front face	0.107	0.147	0.198	0.211
base	0.1476	0.157	0	0
top	0.011	0.0096	0.375	0.4025
underbody	0.00814	0.0073	-0.5387	-0.4319
Partial resultant	0.2737	0.3209	0.0343	0.1816
wheelhouse	-	0.025	-	-0.0905
wheel	-	0.0975	-	0.0998
Resultant	-	0.4434	-	0.1909

2.7.2 Exposed wheel air flow pattern

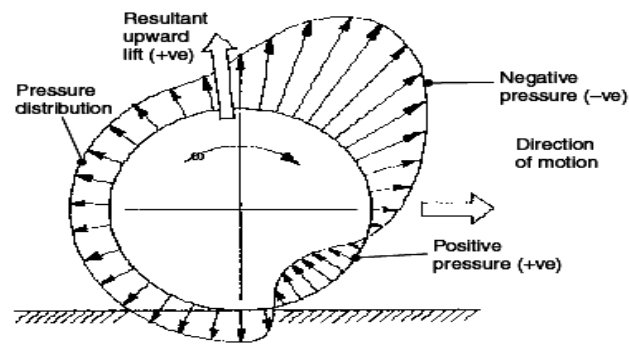
When a wheel rotates some distance from the ground air due to its viscosity attaches itself to the tread and in turn induces some of the surrounding air to be dragged around with it. Thus this concentric movement of air establishes in effect a wheel vortex (Figure 2.10(a)). If the rotating wheel is in contact with the ground it will roll forwards which makes wind tunnel testing under these conditions difficult, this problem overcome by using a supportive wheel and floor rig. The wheel is slightly submerged in a well opening equal to the tyre width and contact patch length for a normal loaded wheel and a steady flow of air is blown towards the frontal view of the wheel. With the wheel rig simulation a rotating wheel in contact with the ground, the wheel vortex air movement interacts and distorts the parallel main airstream.

The air flow pattern for an exposed wheel can be visualized and described in the following way. The air flow meeting the lower region of the wheel will be stagnant but the majority of the airstream will flow against the wheel rotation following the contour of the wheel until it reaches the top. Then it separates from the vortex rim and continues to flow towards the rear but leaving underneath and in the wake of the wheel a series of turbulent vortices shown in Figure 2.10(b). The actual point of separation will creep forwards with increased rotational wheel speed. Air pressure distribution around the wheel will show positive pressure build-up and stagnant air flow front region of the wheel, but this changes rapidly to a high negative pressure where the main air flow breaks away from the wheel rim as in Figure 2.10(c). It then declines to some extent beyond the highest point of the wheel, and then remains approximately constant around the rear wake region of the wheel. Under these described conditions, the exposed rotating wheel produces a resultant positive upward lift force which tends to reduce the adhesion between the tyre tread and ground [15].



(a) Wheel rotation in still air away from the ground

(b) Air flow pattern with wheel rolling on the Ground

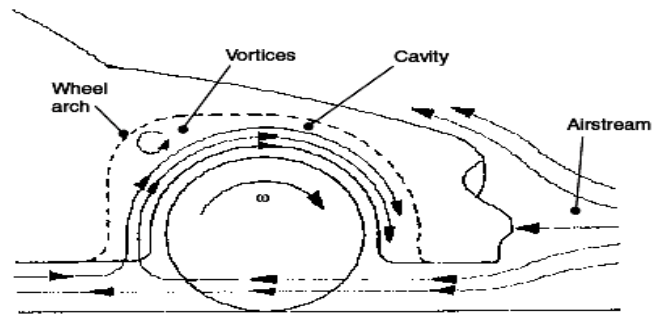


(c) Air pressure distribution with wheel rolling on the ground

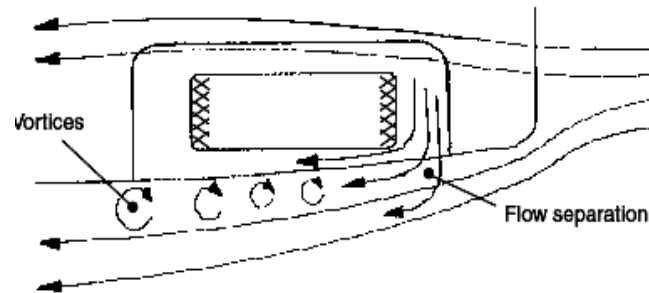
Figure 2.10(a-c): exposed wheel air flow pattern and pressure distribution [15]

2.7.3 Partial enclosed wheel air flow pattern

The air flow passing beneath the front of the car initially moves faster than the main airstream, this therefore causes a reduction in the local air pressure. At the rear of the rotating wheel due to viscous drag air will be scooped into the upper space formed between the wheel tyre and the wheel mudguard arch as in Figure 2.11(a-b). The air entrapped in the wheel arch cavity circulates towards the upper front of the wheel due to a slight pressure build-up and is then expelled through the front end wheel to the mudguard gap which is at a lower pressure in both a downward and sideward direction. Decreasing the clearance between the underside and the ground and shielding more of the wheel with mudguard tends to produce a loss of momentum to the air so that both aerodynamic lift C_D and C_L coefficients, and therefore forces, are considerably reduced as in Figure 2.12(a-b) [15].



(a) Side view



(b) Plane view

Figure 2.11(a-b): Wheel arch air flow [15]

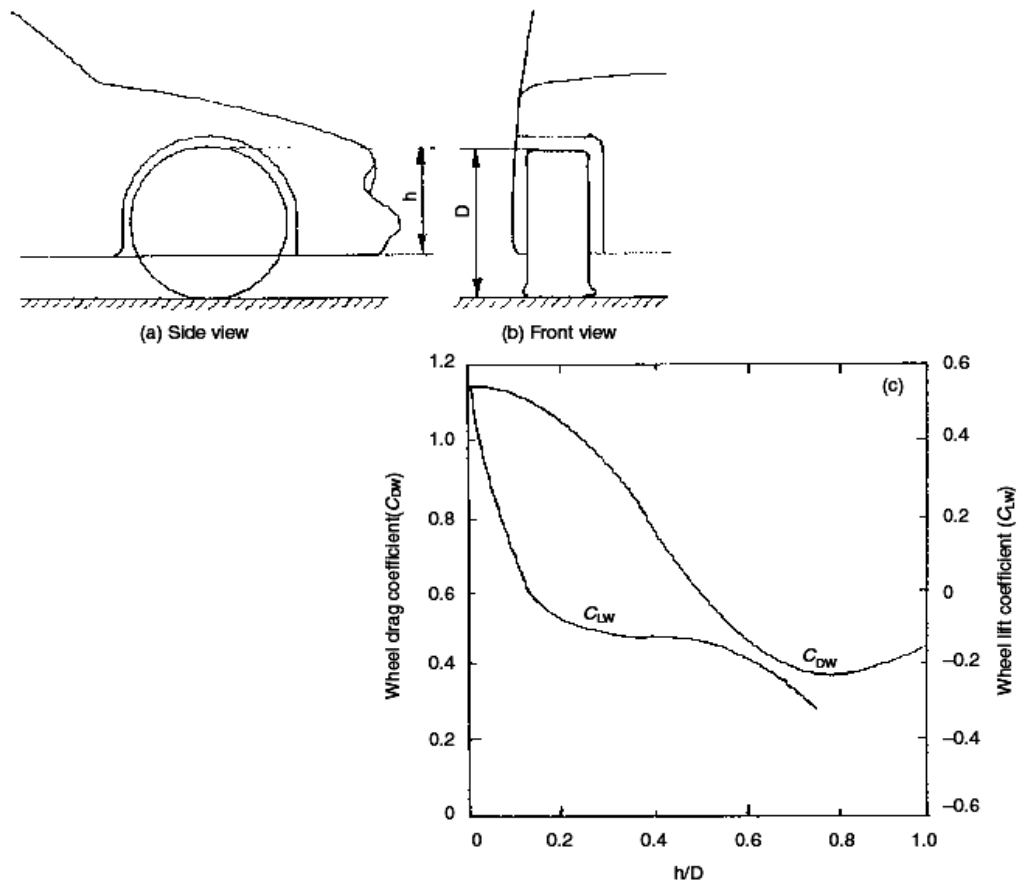


Figure 2.12(a-b): Affect of underside ground clearance on both lift and drag coefficients [15]

2.7.4 Sample of Wheel houses

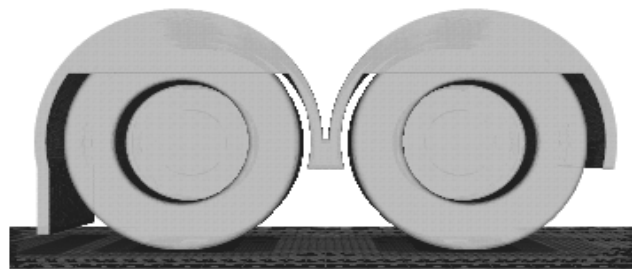


Figure 2.13: Rear wheel cover for lorry [17]



Figure 2.14: Rear wheel cover for Pickup Truck [17]

2.8 Dynamic Fluid Properties

2.8.1 Air Density Properties Related To Vehicle

The air density is variable depending on temperature, pressure, and humidity conditions. The air density must be expressed as mass density, obtained by dividing by the acceleration of gravity. Density at other conditions can be estimated for the prevailing pressure, P and temperature, T conditions by the equation below [2].

The highest speeds achieved by land-vehicles during record attempts are on the order of the speed of sound which is for air, $= 330 \text{ m/s} = 1225 \text{ km/h} = 761.6 \text{ mph}$. In the flow field of a body exposed to such a free stream the compressibility of the air is very important. On the other hand, most vehicles including racing cars are operated at speeds which are lower than one-third of the speed of sound. For this speed range the variations of pressure and temperature in the flow field are small as compared to free-stream values, and therefore the corresponding changes of density can be neglected. Thus the fluid can be regarded as incompressible [2].

2.8.2 Air Viscosity Properties Related To Vehicle

The air will have its own viscosity when the car is moving through the air surrounding. Viscosity is caused by the molecular friction between the fluid particles. It relates momentum flux to velocity gradient, or applied stress to resulting strain rate. According to Newton's law for the flow parallel to a wall, the shear stress, τ is proportional to the velocity gradient du/dy . The constant factor μ is a property of the fluid called dynamic viscosity. In general its value depends on the temperature. Often the quotient $\nu = \mu/\rho$ is used, which is called kinematics viscosity and which depends on pressure and temperature [12]. For incompressible fluids, only temperature dependence exists for ν and μ . The viscosity of a real fluid is the physical reason for the occurrence of a friction drag in the presence of a velocity gradient at a wall. It is same case in surface contact of the vehicle as when the vehicle is moving in any velocity.

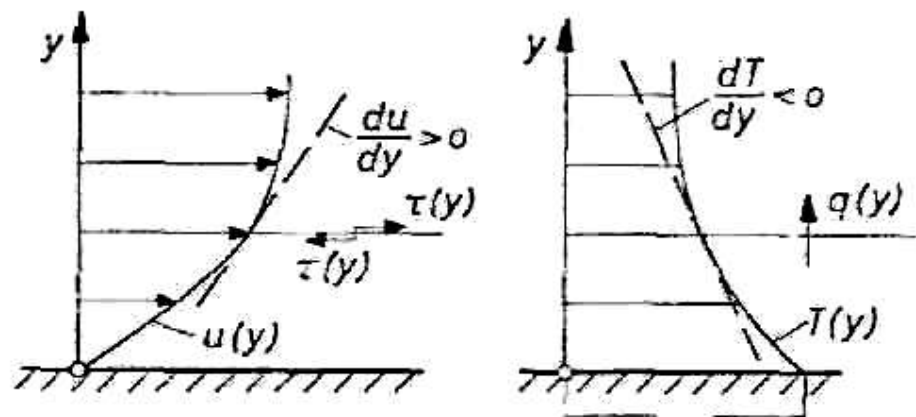


Figure 2.15: Distribution of velocity and temperature in the vicinity of a wall

[12]

2.9 Friction Drag

The pressure in the separation region is below that imposed on the front of the vehicle, and the difference in these overall pressure forces is responsible for 'from drag'. The drag forces arising from the action of viscous friction in the boundary layer on the surface of the car is the "friction drag". In the boundary layer, the velocity is

reduced because of friction [2]. In a viscous fluid a velocity gradient is present at the wall. Due to molecular friction a shear stress acts everywhere on the surface of the body as indicated in Figure 2.15 below. The integration of the corresponding force components in the free-stream direction leads to the so-called friction drag. In the absence of flow separation, this is the main contribution to the total drag of a body in two-dimensional viscous flow.

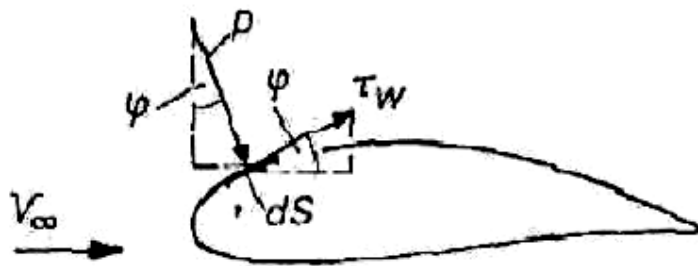


Figure 2.16: Determination of the drag of a body (two-dimensional flow)

2.10 Reynolds Number

$$\text{Reynolds Number} = \frac{\rho \ell v}{\mu}. \quad (2.4)$$

ρ = density of the fluid

ℓ = characteristic of length

v = velocity of the body in the fluid

μ = viscosity of the fluid

The general factors of drag, aerodynamic friction, are density and viscosity of the fluid, air being considered a fluid. The definition of Reynolds Number is shown at above [9]. The Reynolds Number for a body that is large in size and slow in velocity could produce an equivalent Reynolds Number of a very small object that travels with a

high velocity. This seems like it isn't possible logically until we evaluate the definition Reynolds Number and see that it is. At high Reynolds numbers, typical of full-sized car, it is desirable to have a laminar boundary layer. This results in a lower skin friction due to the characteristic velocity profile of laminar flow. At lower Reynolds numbers, such as those seen with model car, it is relatively easy to maintain laminar flow. This gives low skin-friction, which is desirable. However, the same velocity profile which gives the laminar boundary layer its low skin friction also causes it to be badly affected by adverse pressure gradients. As the pressure begins to recover over the rear part of the rear hood, a laminar boundary layer will tend to separate from the surface. Such separation causes a large increase in the pressure drag, since it greatly increases the effective size of the rear hood section [9].

2.11 Fuel Consumption

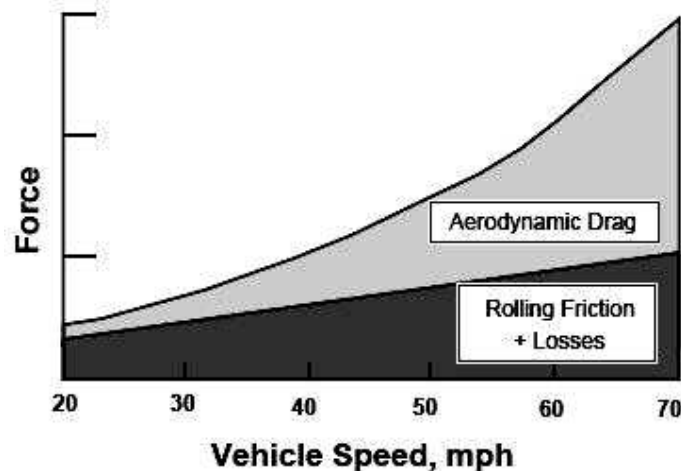


Figure 2.17: Graphic depicting representative horsepower requirements versus vehicle speed for a heavy vehicle tractor-trailer truck [13]

Aerodynamics devices will reduce the drag and also will improve the fuel economy of moving vehicle. Drive-train losses, rolling friction, and aerodynamic drag are contributed for the primary resistance forces that influenced of energy usage. The chart of figure 2.16 shows that as vehicle speed is increased the force required to overcome both aerodynamic drag and rolling friction increases. However, the rate of

increase in aerodynamic drag with increasing vehicle speed is much greater than that for rolling friction such that at approximately 50 mph the force directed at overcoming aerodynamic drag exceeds that required to overcome rolling friction [13]. These data do not take into account several operational and environmental factors that can have a dominating effect on the aerodynamic drag of moving vehicle. The chart also shows that if the average speed approaches 30 mph then it is nearly impossible to achieve a 10% improvement in fuel economy through aerodynamic drag reduction. It shows that in higher speed will achieve the 10% of improvement in fuel economy.

A number of additional factors such as interference from other vehicles, atmospheric effects, and road conditions are the factors that must be addressed when developing technologies to improve the fuel economy of vehicles. These efforts of adding the aerodynamics devices have produced reductions in the aerodynamic drag of 30%, for an operating speed of 60 mph, with corresponding improvements in fuel economy approaching 15%. An assessment of the aerodynamic drag indicates that the reduction in aerodynamic drag at 60 mph would be closer to 20%, which corresponds to a 10% improvement in fuel economy.

This improvement in fuel economy correlates to an equivalent drag reduction of approximately 30% with a corresponding drag coefficient of 0.45. Note, the aerodynamic drag reduction and associated fuel savings also result in a measurable reduction in exhaust emissions that is equivalent to the percent reduction in fuel usage. The application of the subject aerodynamic drag reduction technologies to trucks and similar high drag vehicles offers additional synergistic benefits such as the ability to use of alternate lower-energy fuels and the use of alternate power sources.

2.12 Result Validation in literature

Flow past a simplified vehicle model with wheelhouse and stationary wheel and ground was investigated by the first author [17] in a wind tunnel with flow visualization by using the oil-film method. Flow past the same arrangement (geometry, Reynolds number, boundary conditions) was also calculated. The results of flow visualization and

simulation are compared in Fig. 4.5. The qualitative agreement of the observed oil-film pattern and wall shear stress lines (streak lines) is quite good, reinforcing the reliability of the CFD simulation used.

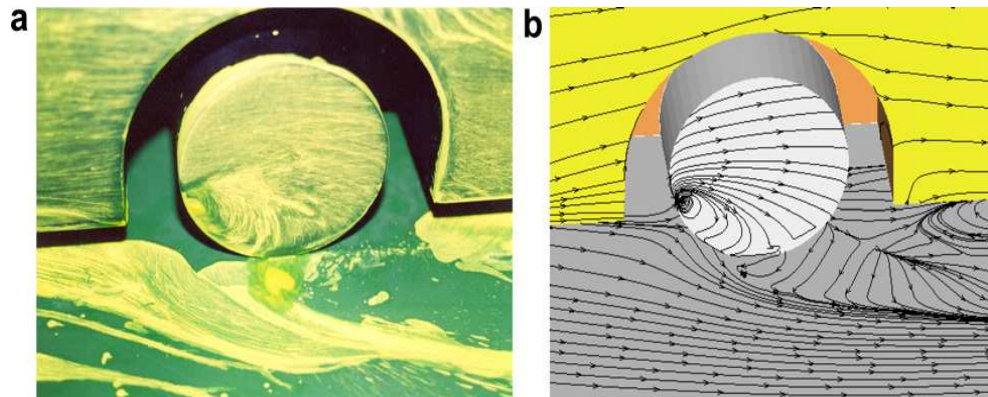


Figure 2.18: Flow at a stationary wheel and ground: (a) oil-film visualization in wind tunnel; (b) numerical simulation (wall streak lines) [17]

Table 2.4: Experimental and CFD values for drag and lift coefficient of the wheel of Fabijanic's vehicle model with rear wheel cover [17]

	C_L	C_D
Experiment	0.250	0.360
CFD (authors')	0.254	0.366
Difference ΔC	0.004	0.006

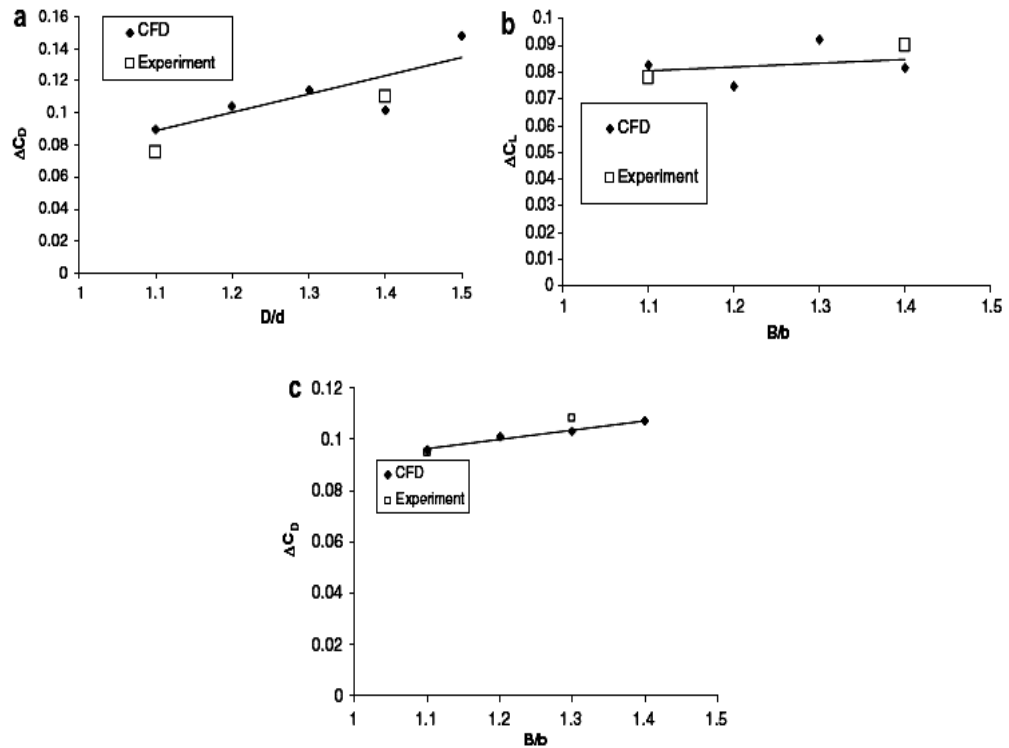


Figure 2.19: Comparison of numerical parameter studies with experimental ones [17]

It is confirm that application of rear wheel cover will cause the airflow on the model at different speed compared to model without rear wheel cover. The simulation result and analysis result by previous researcher of rear wheel cover in term of drag coefficient value is almost have the same pattern.

CHAPTER 3

METHODOLOGY

3.1 Introduction

The objective of the project can be achieved by setting the methodology in well. This will make the project is cable of complete on time. This chapter will explain the detailed about the methodology progress during Final Year Project 1 and 2. This chapter will list all the method that included and relevant to complete the project. The title was given by the supervisor in the beginning of this semester with the title “Design and Analysis Rear Diffuser for HEV Model”. The detailed related literature review was informed acquired the important things in the Chapter 2.

The project will analyze the affect of rear diffuser on the car based on the pressure, velocity and drag. Computational Fluid Dynamic (CFD). Cosmos flow will be used to analyze the drag coefficient reduction by rear wheel cover. This software will make the objective to be achieved successfully. To solve all the problem, first thing to do is to determine all the flow works with the duration of time, the Gantt chart is a recommended method to use. So that all the flow work with the description of works were carried out to meet the date line.

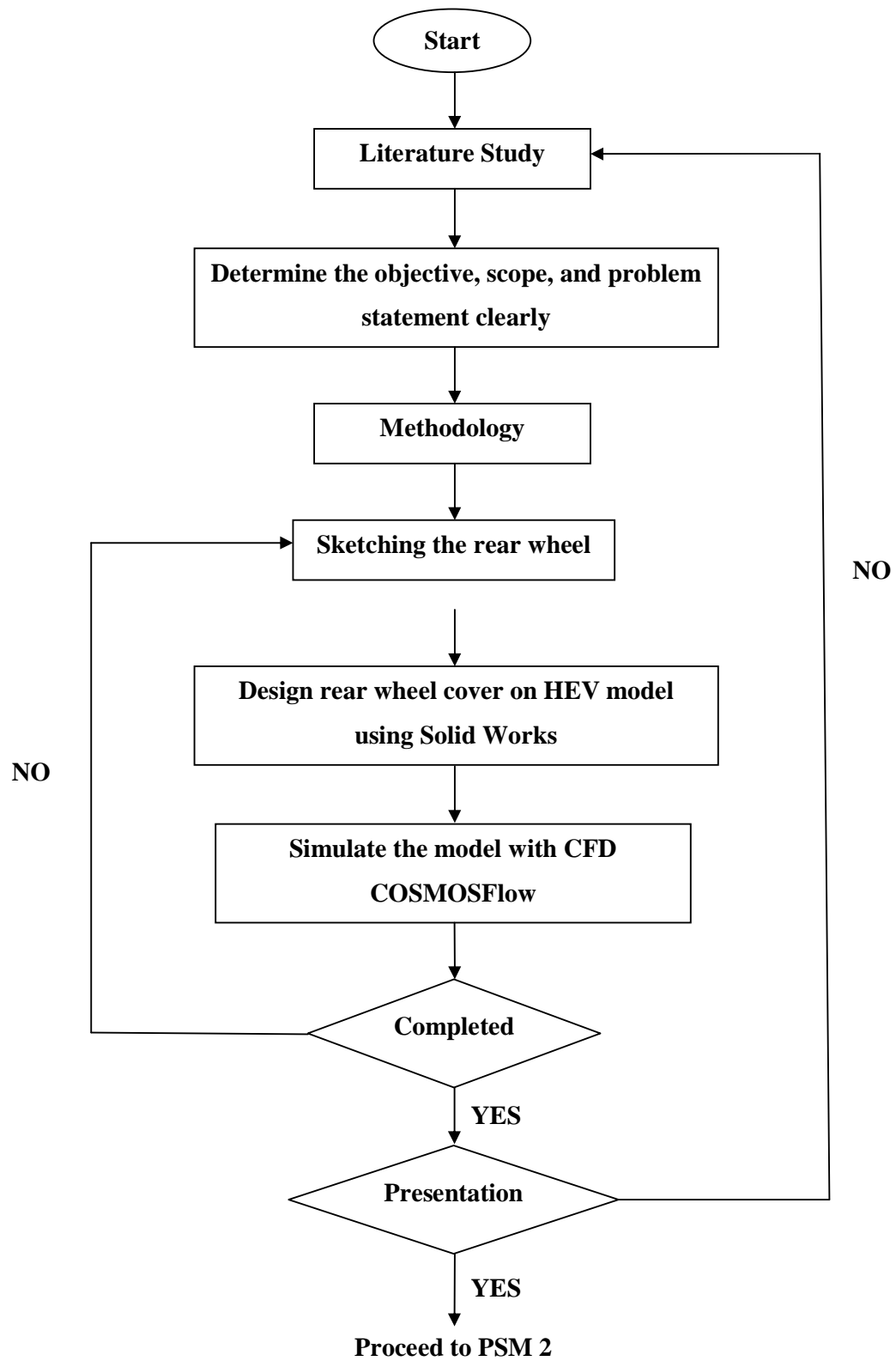


Figure 3.1: Methodology flow chart for PSM 1

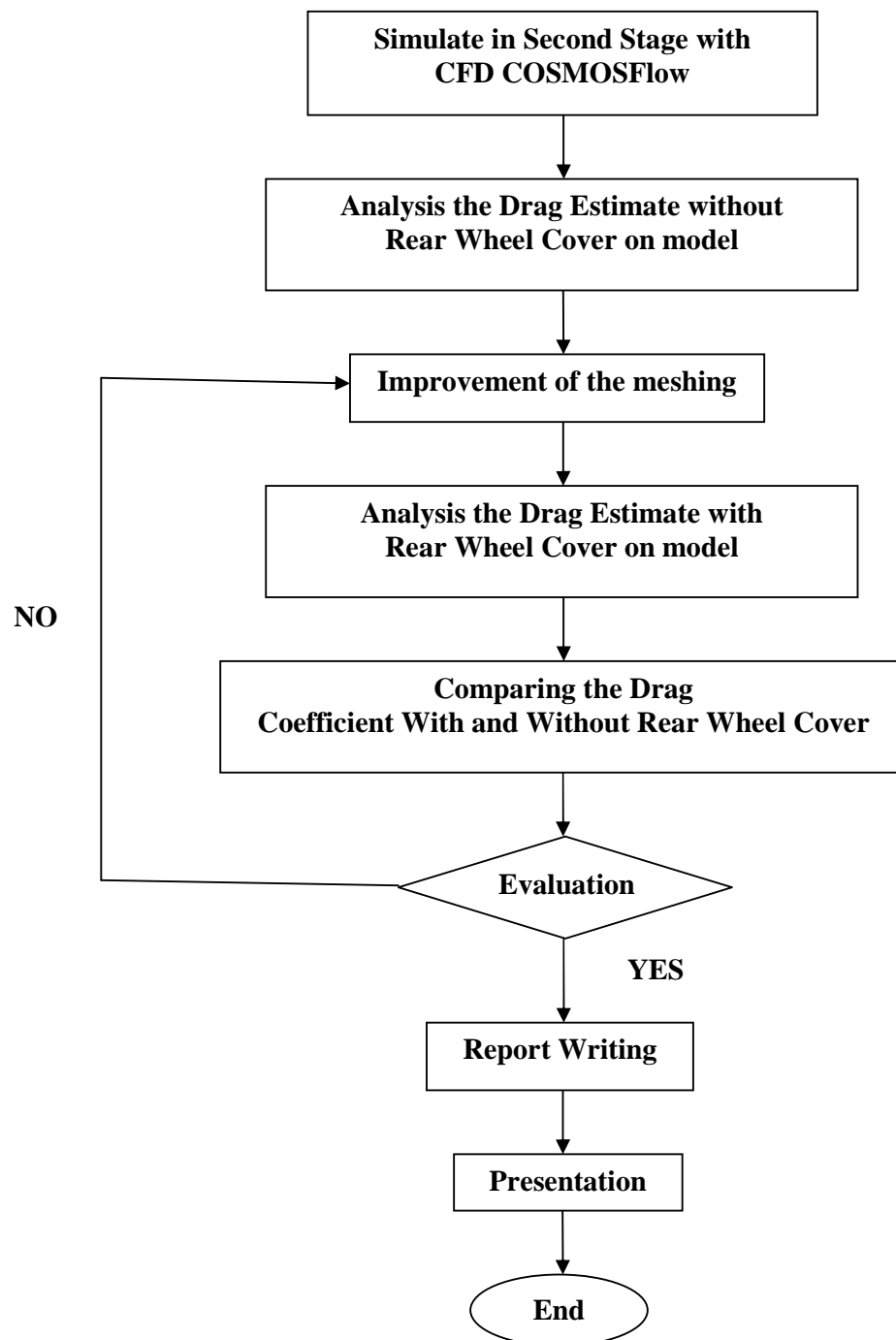


Figure 3.2: Methodology flow chart for PSM 2

3.2 Problem Solving

By referring to this project, the main problem solving is by using the Computational Fluid Dynamics to analyze the flow velocity and pressure distribution around the car body, to complete that there must be a problem solving method or flow to complete that. So, the works are regarding to this solving problem must be more organize. With referring to the methodology flow chart, the detail for each activity can be referring to next sub topics.

3.2.1 Literature Study

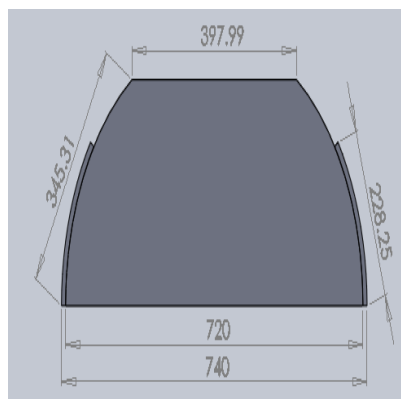
This project is start with literature review and research from the internet, company websites, market survey, books and journal about the title. This stage is very important to make a literature study about the basic of the aerodynamics such as a flow characteristic around the vehicles , drag coefficient, lift , pressure distribution and others fluid dynamics requirement. In this part, the detail about the design of the rear diffuser and all the effect about the external flow of the HEV model will be explained. The literature study was continued from the beginning of this project so that all the latest information will be updated from the time to time. This part also can give the individual to understand what the important things needed before proceed to the next stage.

3.2.2 Identify Project Objectives

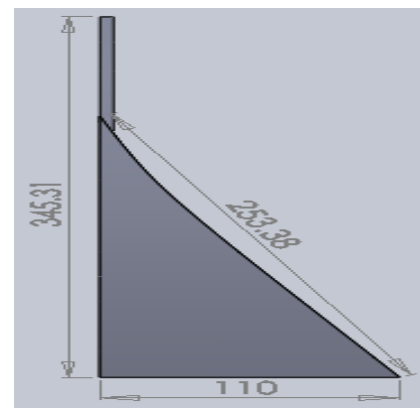
Objective is the most important part in this project. By the determination of the objective, the project will clearly see what will be doing from the beginning. The problem that will occur at the rear end of the car must be analyzed. This is very important so that the target objective from the starting can be achieved. The scopes of this project can be done after determine the objective. This will help the project to progress smoothly and can be success.

3.2.3 Measurement the Rear Wheel Cover

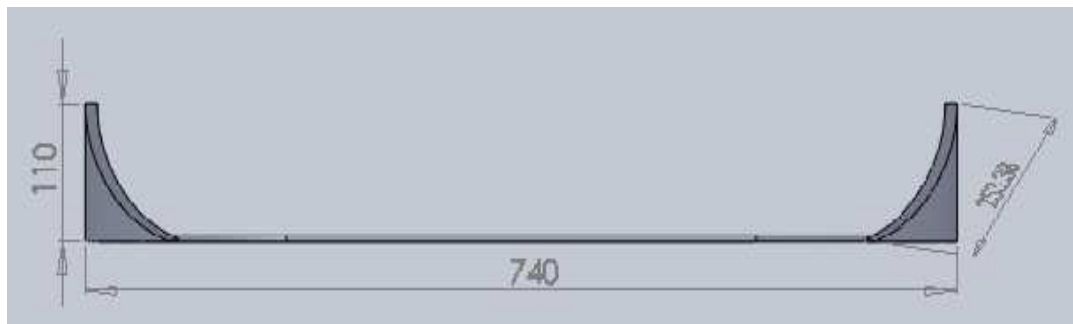
Before the analysis of this project, the rear wheel cover model is requiring to get the dimension. From the literature study, the rear wheel cover is installing at the right and left side of the model. The dimension of the rear wheel cover are limited because the area of the rear tyre opening. Figure 3.3(a-c) below are the dimension of the rear diffuser in different view.



(a) Front view



(b) Right View



(b) Bottom View

Figure 3.3: Basic view of the rear Wheel Cover from different side of view

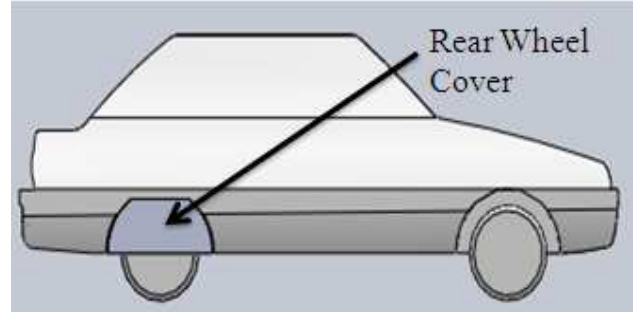


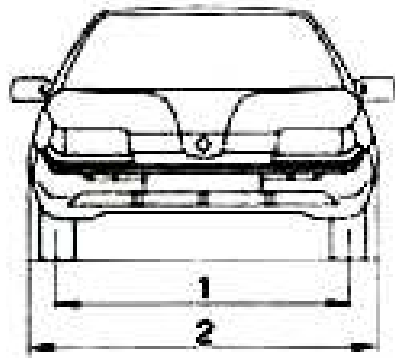
Figure 3.4: Rear wheel cover on the HEV model

3.2.4 Dimension of the HEV Model

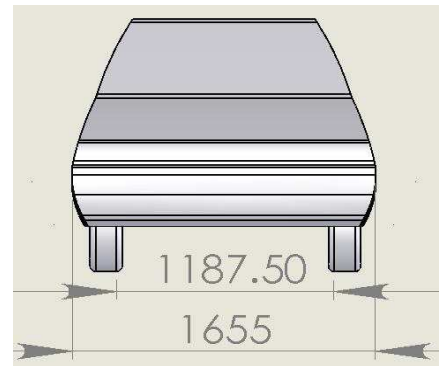
The car model that will be use on this project is basically a Proton Iswara Aeroback. The car model are get from the supervisor, all the dimension are already taken by the previous student that doing the aerodynamic devise on this car model. The dimensions are taken from the Proton Manuals Book and from that dimension; the car was transferred into a 3-D modeling by using the Solid Works software.

3.2.5 3-D Car Modeling

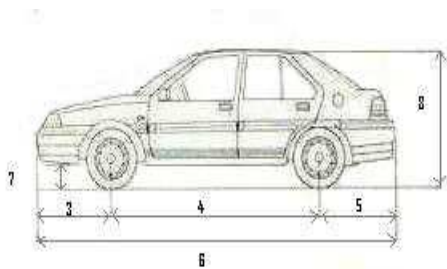
HEV model was modeling and transferred into a 3-D modeling using the Computational Aided Design (CAD). The model is modeling by referring the true dimension from the Proton Manuals Book. The model of rear wheel cover is added to this 3-D model at the rear wheel houses to complete the CFD simulation. The model dimension and actual vehicle dimension is not quite match. This is because some detailing such as a fender, underbody, front and rear bumper of the vehicle were made by using the assumption that will only fits the model. This is the important things to carry out for the simulation result. All the part that has been mention at above, the part is modeled together with the body because the project is focusing on the external flow only. The dimension is not accurate from the real measurement from the Proton Manual Book.



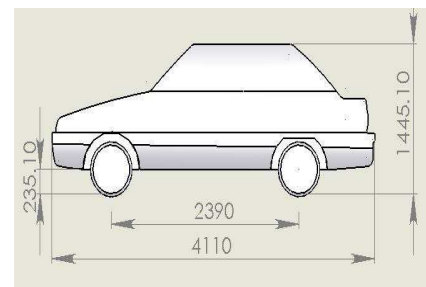
(a) Front View



(b) Front View

Figure 3.5: (a) Manual drawing from the data sheet, (b) 3-Dimensional drawing

(a) Side View



(b) Side View

Figure 3.6: (a) manual drawing from the data sheet, (b) 3-Dimensional drawing

3.2.6 Sketching Applying For Model Improvement

The dimension of the rear wheel cover is installing directly into the HEV model by using the Solid work software. Figure below is the HEV model with the rear wheel cover at the side view.

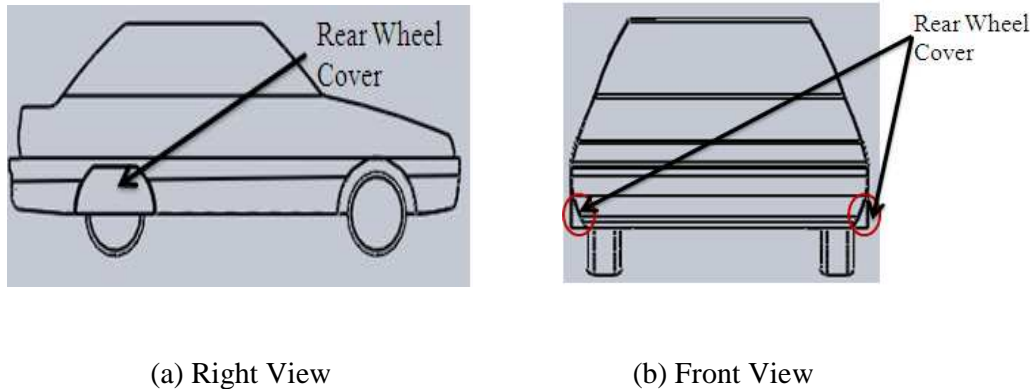


Figure 3.7: Model view with rear wheel cover

3.2.7 CFD Simulation

After the HEV car modeling on CAD, the model will be transfer into a CFD Simulation known as Computational Fluid Dynamics Simulation. The process will make an analysis about the flow velocity and the pressure distribution over the car model body. In this simulation also can determine the laminar and turbulent flow over the car body. The drag can be determined after the setting of the goals. The HEV car model with rear wheel cover is used as the model for the all analysis. With this model, the simulation will be running by using the CFD software. Figure 3.6 below show the boundary condition of the HEV car model with rear wheel cover on CFD.

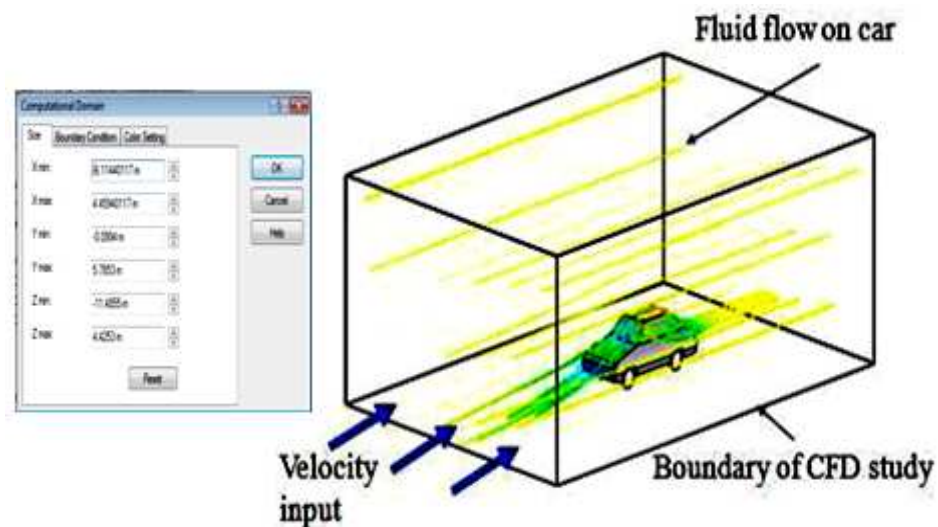


Figure 3.8: CFD boundary condition with streamlines and Computational Domain size

This CFD simulation will be used for determine the flow over the car before and after adding the rear wheel cover to see the difference. This method of CFD simulation is depending on the model, every little aspect will affect the result. This simulation is focusing on the external flow of the vehicles and the effect of the velocity and pressure distribution after given a desired input.

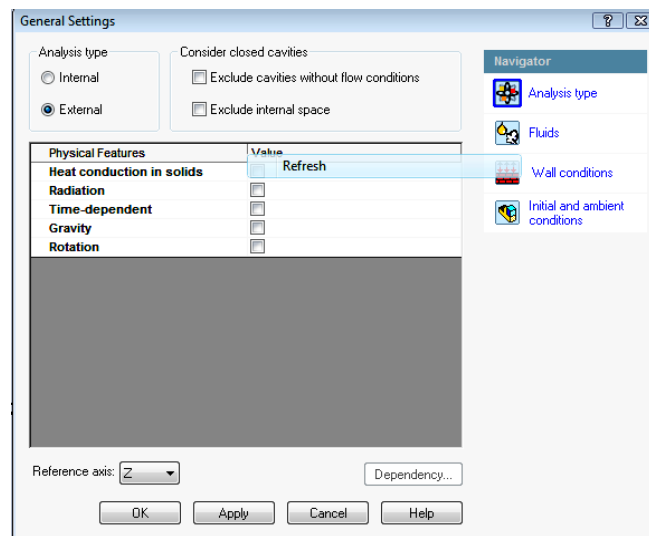
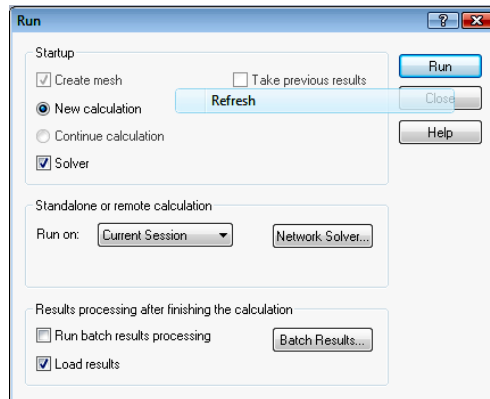


Figure 3.9: Simulation of analysis type

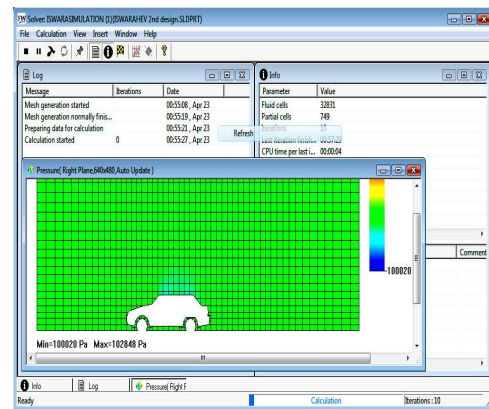
The location of the most laminar and turbulent flow of the vehicles and the most pressure distribution will be shown when a different velocity is given to the vehicles according to the changes from the lower velocity to the maximum velocity. The setting velocities are set 40, 60, 80, 100, 120 and 140 km/h. During this simulation also, all the data will be recorded and the graph of the analysis will be compared after all the simulation is archive.

Air is taking as a fluid for project analysis that surrounding the whole car model in the simulation. The flow characteristic value is a laminar and turbulent; these types of flow will be considered for the simulation. Setting goals are very important to find the drag force. After the solver was finished done, can get the drag force in COSMOSFlow by choose the average force acting on the Z axis. For the refinement, the level taking is

level 4 and the three points that taking for the table of refinement is 10, 20 and 50. The unit in refinement is iterations. The mesh display is needed to show at COSMOSFlow parameter before the running of simulation. The mesh taken is about between courses and fine value. Refer Mesh Independent Analysis (3.2.8) for further information regarding the refinement chosen.



(a) Run Simulation



(b) Analysis Solver

Figure 3.10: (a) Run startup for simulation, (b) Velocity analysis solver for each speed

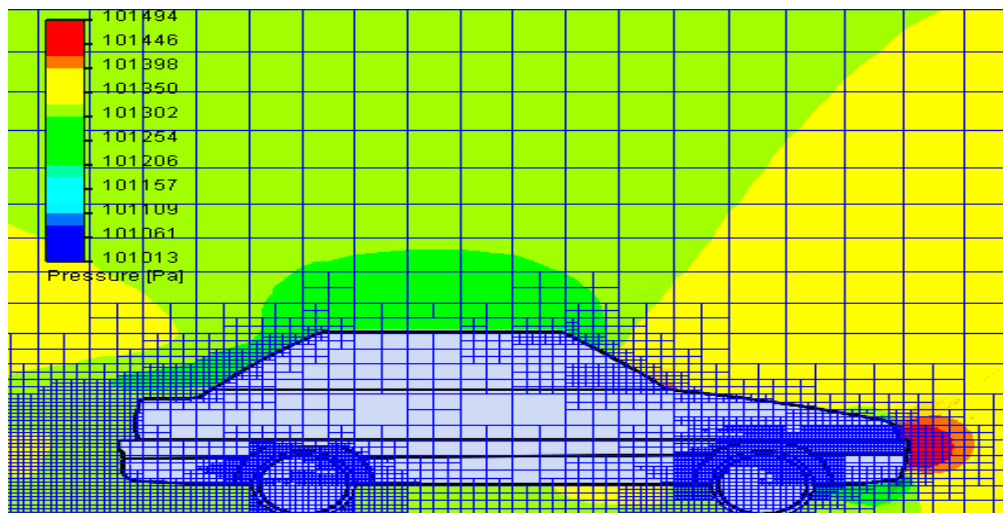


Figure 3.11: CFD Pressure Result Simulation on model

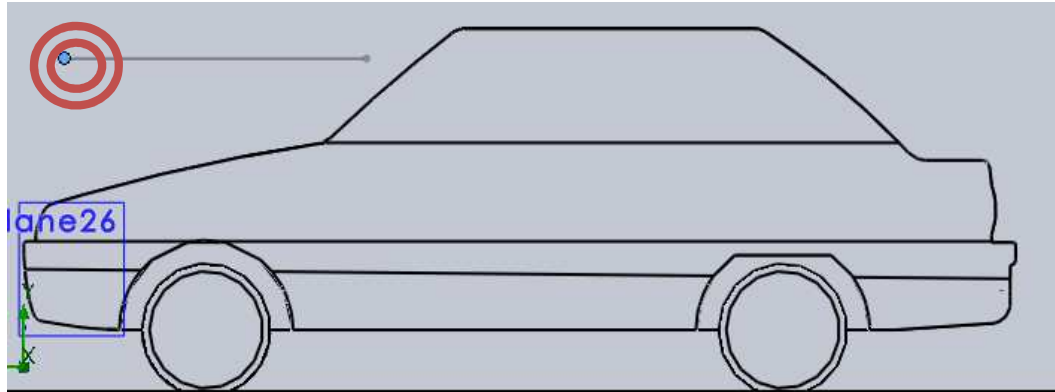


Figure 3.13: Velocity Point for mesh study

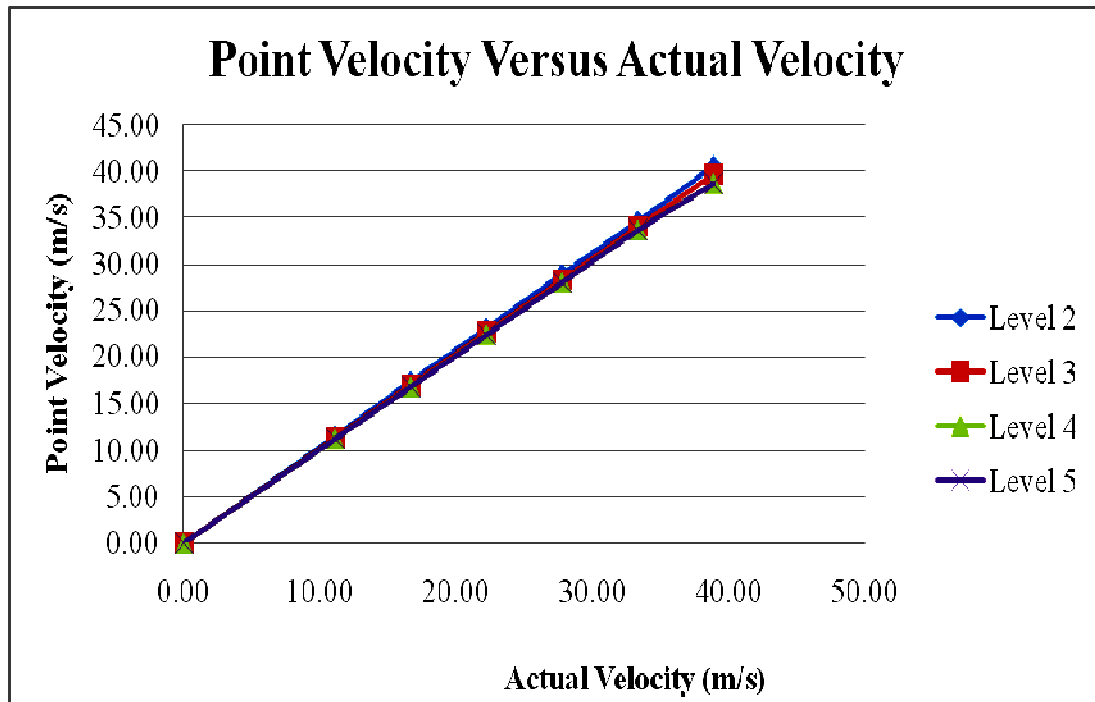


Figure 3.14: Point velocity versus Actual velocity for the model

From the graph above known that the point velocity and the actual velocity value are similarly same at the level 4. So level 4 is choose for the simulation analysis. Some more the time taken was less than level 5.

Table 3.1: Number of cells for each level for the model simulation

	Level 2	Level 3	Level 4	Level 5
Fluid Cells	3516	60301	191775	194222
Solid Cells	1161	6949	24323	25554
Partial Cells	2469	9687	51850	35779
Total Cells	38766	76937	250700	255555
CPU time	1355s (22min)	4729s (1hr 18 min)	16981s (4 hours 42min)	691200s (8hours 24 min)

CHAPTER 4

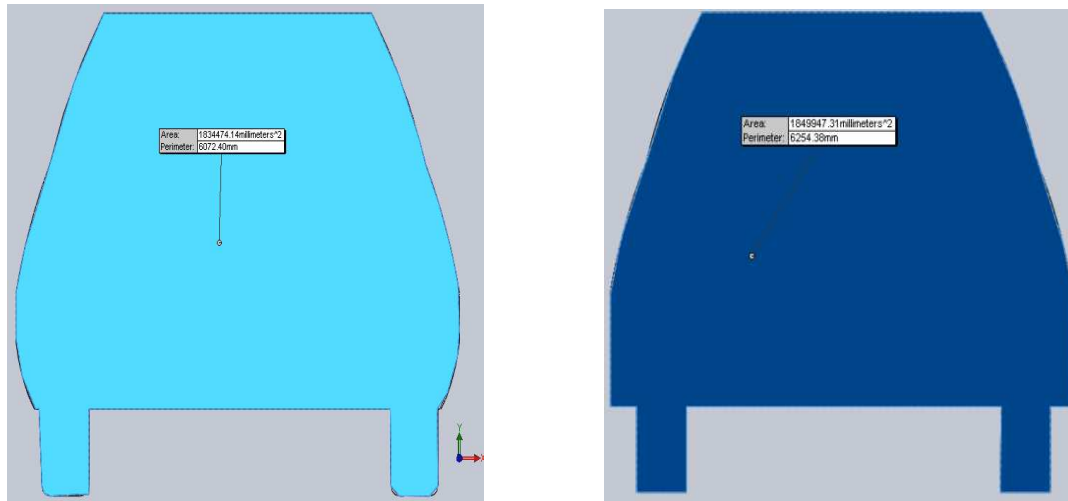
RESULT AND DISCUSSION

4.1 Introduction

The main objective of this project is about to study the effect of rear wheel cover on pressure and velocity distribution. The effect will be simulated before and after the adding of rear wheel cover using the CFD simulation. In automotive design studies, the aerodynamic devices such as rear wheel cover are the important part in designing a vehicle. This aerodynamic device will influence of the stability, performance, fuel consumption and others on the vehicle.

Nowadays, there are many new vehicle model are install the rear wheel cover device. In this project analysis will show the result when adding the rear wheel cover at the rear vehicle and will compare with the vehicle model without the rear wheel cover. The adding of rear wheel cover is the main characteristics that were taken into consideration in the analysis. By mean, this is also one of the ways how a designer of the most leading world performance car manufacturer produce this rear wheel cover as their standard part for the vehicles as their standard kits. This CFD simulation analysis will determine there is any changing and improvement before and after the rear wheel cover device are install at the vehicle model.

4.2 Frontal Area of the Model



(a) Without Rear Wheel Cover

(b) With Rear Wheel Cover

Figure 4.1(a-b): The frontal area without and with rear wheel cover from the Solid Works

From the figure above the frontal area for the model without rear wheel cover is $A = 1.834 \text{ m}^2$ and with rear wheel cover is $A = 1.845 \text{ m}^2$.

4.3 Drag Coefficient

The drag coefficient can be calculated by using the drag force equation. From the value of drag force that obtains in COSMOSFlow analysis, the drag coefficient, C_D can be determined. The drag coefficient will be calculated with the equation 2.3. The velocity used is from 40 km/h until 140 km/h.

Determine the C_D for model with rear wheel cover at velocity 140 km/h. From the data given,

$$F_D = 699.4342 \text{ N}$$

$$\rho = 1.225 \text{ kg/m}^3$$

$$A = 1.845 \text{ m}^2$$

$$V = 38.89 \text{ m/s}$$

Solution,

$$C_D = \frac{699.4342 \text{ N}}{\frac{1}{2}(1.225 \text{ kg/m}^3)(38.89 \text{ m/s})^2 (1.845 \text{ m}^2)}$$

$$= 0.4093$$

Determine the C_D for model without rear wheel cover at velocity 140 km/h. From the data given,

$$F_D = 697.4401 \text{ N}$$

$$\rho = 1.225 \text{ kg/m}^3 \text{-----[15]}$$

$$A = 1.834 \text{ m}^2$$

$$V = 38.89 \text{ m/s}$$

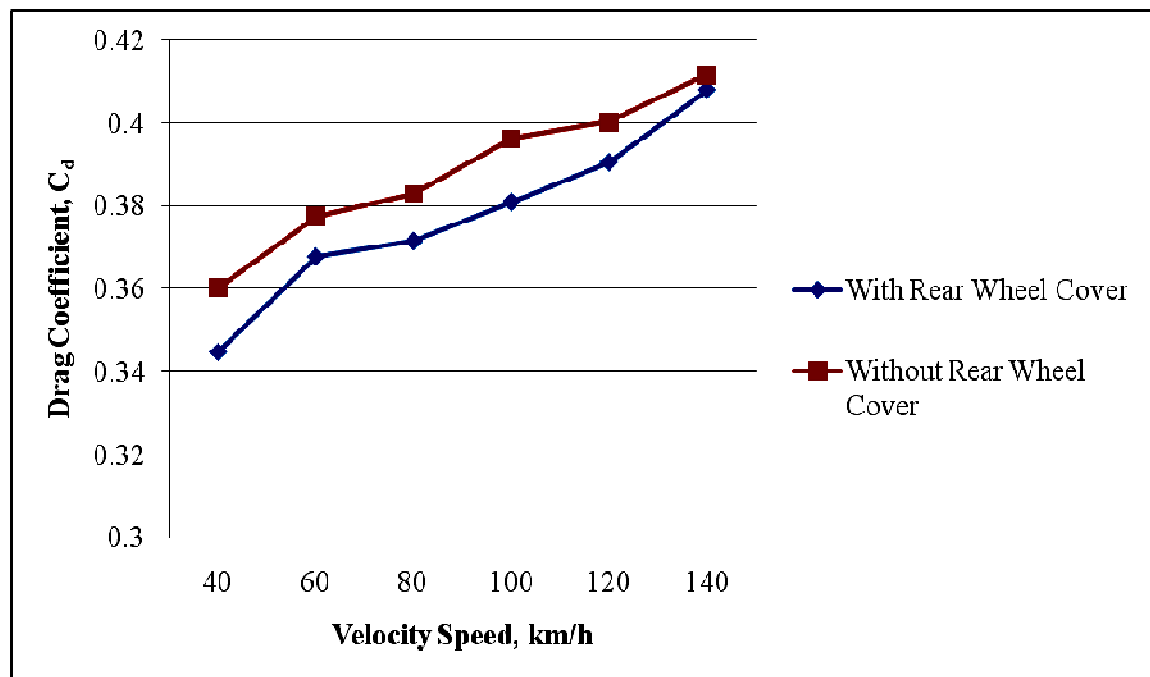
Solution,

$$C_D = \frac{697.4401 \text{ N}}{\frac{1}{2}(1.225 \text{ kg/m}^3)(38.89 \text{ m/s})^2 (1.834 \text{ m}^2)}$$

$$= 0.4105$$

Table 4.1: Drag coefficient of vehicle with and without rear wheel cover

Velocity Speed, km/h	Drag Force, F_D [N]		Drag Coefficient, C_D	
	With Rear Wheel Cover	Without Rear Wheel Cover	With Rear Wheel Cover	Without Rear Wheel Cover
40	48.0985	49.9621	0.3448	0.3603
60	115.4470	117.8046	0.3678	0.3775
80	207.4007	212.4209	0.3716	0.3829
100	332.1754	343.5190	0.3810	0.3963
120	490.4545	499.6173	0.3906	0.4003
140	697.4401	699.4343	0.4081	0.4117

**Figure 4.2:** Drag coefficient vs. Speed

The Figure 4.2 show the drag coefficient related with the vehicle speed. The different lines of the drag coefficient with and without rear wheel cover are plotted. When the changing of the velocity, the higher C_D is obtained and the flow contour also change. By this analysis, increasing value of speed will make the drag of the vehicle increase too. By adding the rear wheel cover, the maximum drag at high speed will be reduced for reducing the fuel consumption usage. The drag coefficient of model without rear wheel cover is higher than model with rear wheel cover. By compare with and without the rear wheel cover, the drag coefficients of model with rear wheel cover are decrease. This is because rear wheel cover will reduce the wake region area at the side of the model wheel houses. Drag will be reduced when the wake region are decrease. At the high speed only will show the effect of adding the rear wheel cover to the model. This has shown at the graph above. From the graph of drag coefficient versus speed above, the increasing of C_D is slightly proportionally with the increasing of speed. The higher speed of vehicle will give higher drag coefficient due to higher drag force to overcome as the vehicle moving. The minimum C_D obtained at the speed of 40 km/h is 0.3448 and the maximum value of C_D obtained at the speed of 140 km/h is 0.4117. The average C_D for model without rear wheel cover is 0.3882 and for the model with rear wheel cover is 0.3773.

4.4 Aero Power

The aero power can be calculated by using the aero power equation from the study. From the result value of drag coefficient that obtains in drag coefficient equation, aero power, P can be determined. The aero power will be calculate with the equation at the below.

$$P = \rho / 2 C_D A V (V + V_o)^2 \quad (4.1)$$

P = Aero power [W]

ρ = air density [kg/m³]

C_D = drag coefficient

A = vehicle section area [m²]

V = velocity [m/s]

V_o = wind velocity [m/s]

Determine the P for model with rear wheel cover at velocity 140 km/h. From the data given,

$$\rho = 1.225 \text{ kg/m}^3$$

$$C_D = 0.4081$$

$$A = 1.845 \text{ m}^2$$

$$V = 38.89 \text{ m/s}$$

$$V_o = 0 \text{ m/s}$$

Solution,

$$P = \frac{1.225 \text{ kg/m}^3}{2} (0.4093) (1.845 \text{ m}^2) (38.89 \text{ m/s}) (38.89 \text{ m/s} + 0 \text{ m/s})^2$$

$$= 27.1227 \text{ kW}$$

Determine the P for model without rear wheel cover at velocity 140 km/h. From the data given,

$$\rho = 1.225 \text{ kg/m}^3$$

$$C_D = 0.4117$$

$$A = 1.834 \text{ m}^2$$

$$V = 38.89 \text{ m/s}$$

$$V_o = 0 \text{ m/s}$$

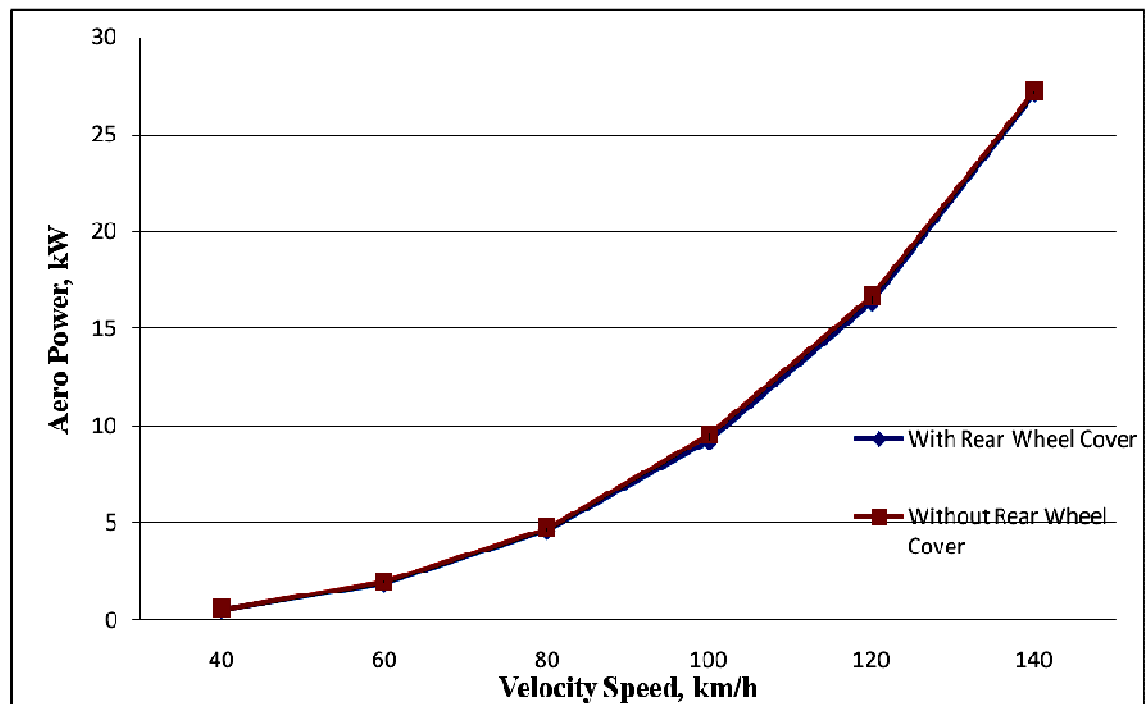
Solution,

$$P = \frac{1.225 \text{ kg/m}^3}{2} (0.4117) (1.834 \text{ m}^2) (38.89 \text{ m/s}) (38.89 \text{ m/s} + 0 \text{ m/s})^2$$

$$= 27.2002 \text{ kW}$$

Table 4.2: Aero power of vehicle with and without rear wheel cover

Velocity Speed, km/h	Aero Power, kW	
	With Rear Wheel Cover	Without Rear Wheel Cover
40	0.5344	0.5551
60	1.9241	1.9634
80	4.6089	4.7204
100	9.2271	9.5422
120	16.3485	16.6539
140	27.1227	27.2002

**Figure 4.3:** Aero power vs. Speed

The figure show the aero power related with the vehicle speed. Vehicle with high speed will use the higher power to make the vehicle move. By using the higher

power, the amounts of the fuel used also are higher. The higher fuel consumption will make the usage of vehicle are not economical. At the low speed, the power are used is still lower compare when at high speed. It will show the difference at 100 km/h and above of vehicle speed in term of power usage. Rear wheel cover device will reduce the amount of power usage. By reduced the amount of power usage, the fuel consumption usage also will lower. This is the economical of fuel usage when adding the rear wheel cover on the vehicle. From the graph, model without rear wheel cover are show the higher of power that is 27.2002 kW compare to the model with rear wheel cover that is 27.1227 kW. With comparing the different analysis data for the 140 km/h its shows around 0.0075 kW of aero power reduced by adding rear wheel cover. From this fuel consumption usage also will reduce.

4.5 Percentage Reduction

From the adding of rear wheel cover on the model, the reduction of drag coefficient, C_D and aero power, P will obtain. This reduction showed the good benefit of adding rear wheel cover on the vehicle. The reductions are calculated in percentage. The average values are used to calculate the percentage of reduction. The percentage reduction will be calculate with the equation at the below.

$$\% \text{ reduction} = \frac{\text{Average Without} - \text{Average with}}{\text{Average without}} \times 100\% \quad (4.2)$$

Table 4.3: Average values of C_D and P

	Average value	
	With Rear Wheel Cover	Without Rear Wheel Cover
Drag Coefficient, C_D	0.3773	0.3882
Aero Power, P	9.9610 kW	10.1059 kW

4.5.1 Percentage of Drag Coefficient Reduction

$$\begin{aligned} \% \text{ reduction} &= \frac{0.3882 - 0.3773}{0.3882} \times 100\% \\ &= 2.8078 \% \end{aligned}$$

The range for C_D reduction is estimate to be up than 2.8078 %.

4.5.2 Percentage of Aero power Reduction

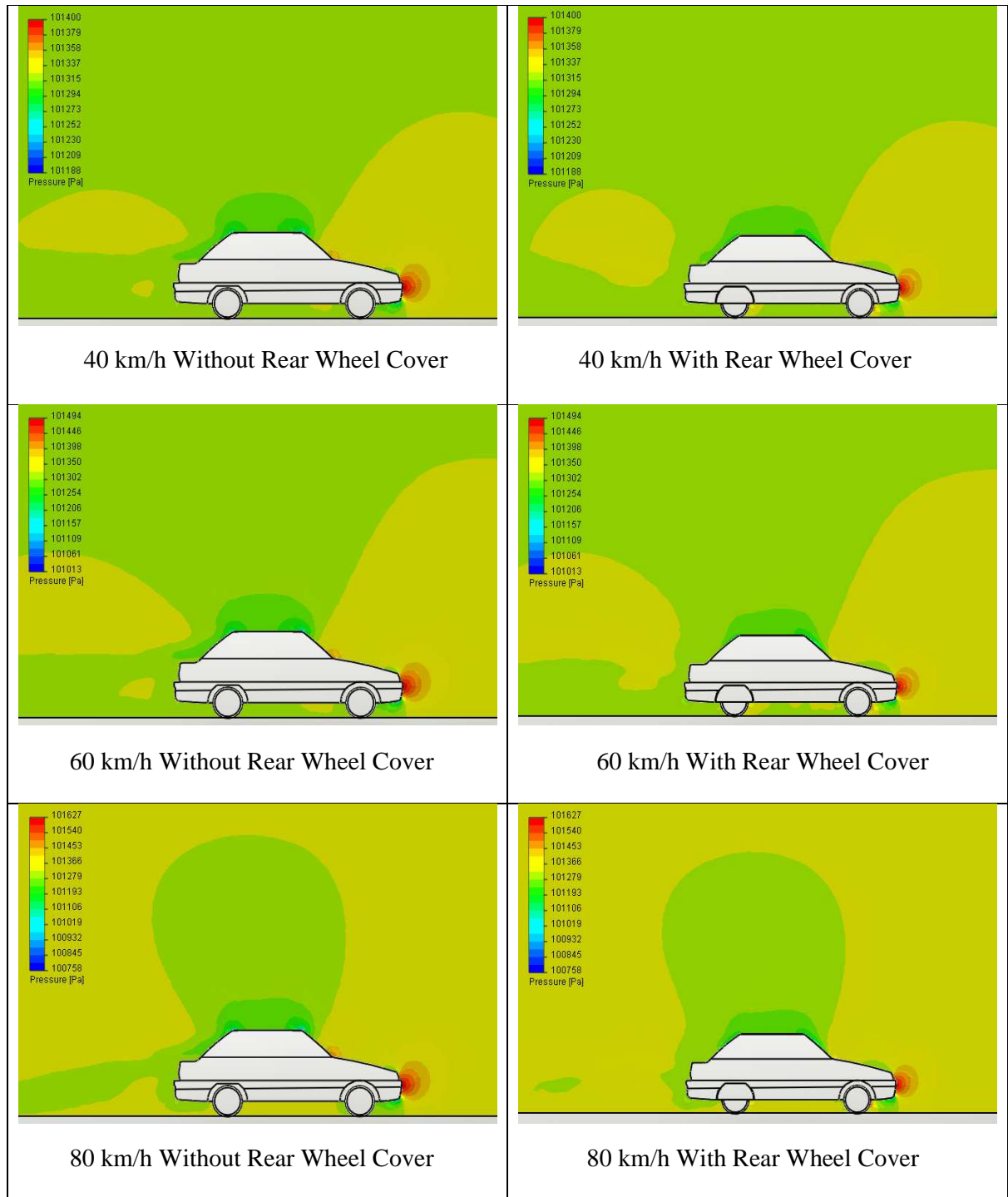
$$\begin{aligned} \% P \text{ reduction} &= \frac{10.1059 \text{ kW} - 9.9610 \text{ kW}}{10.1059 \text{ kW}} \times 100\% \\ &= 1.4338 \% \end{aligned}$$

The range for P reduction is estimate to be up than 1.4338 %.

4.6 Simulation Result

The simulation result shows the final result for both conditions. The first condition is where the HEV model is in a standard condition without an addition of rear wheel cover. The second condition is where the HEV model is an addition of rear wheel cover. Any aerodynamic devices such as front spoiler, vortex generator, rear spoiler, rear wheel cover and more do have an effect on overall flow of the vehicles. The different velocity will give the different result of simulation because of the changing of Re .

4.6.1 Simulation of External Pressure Distribution



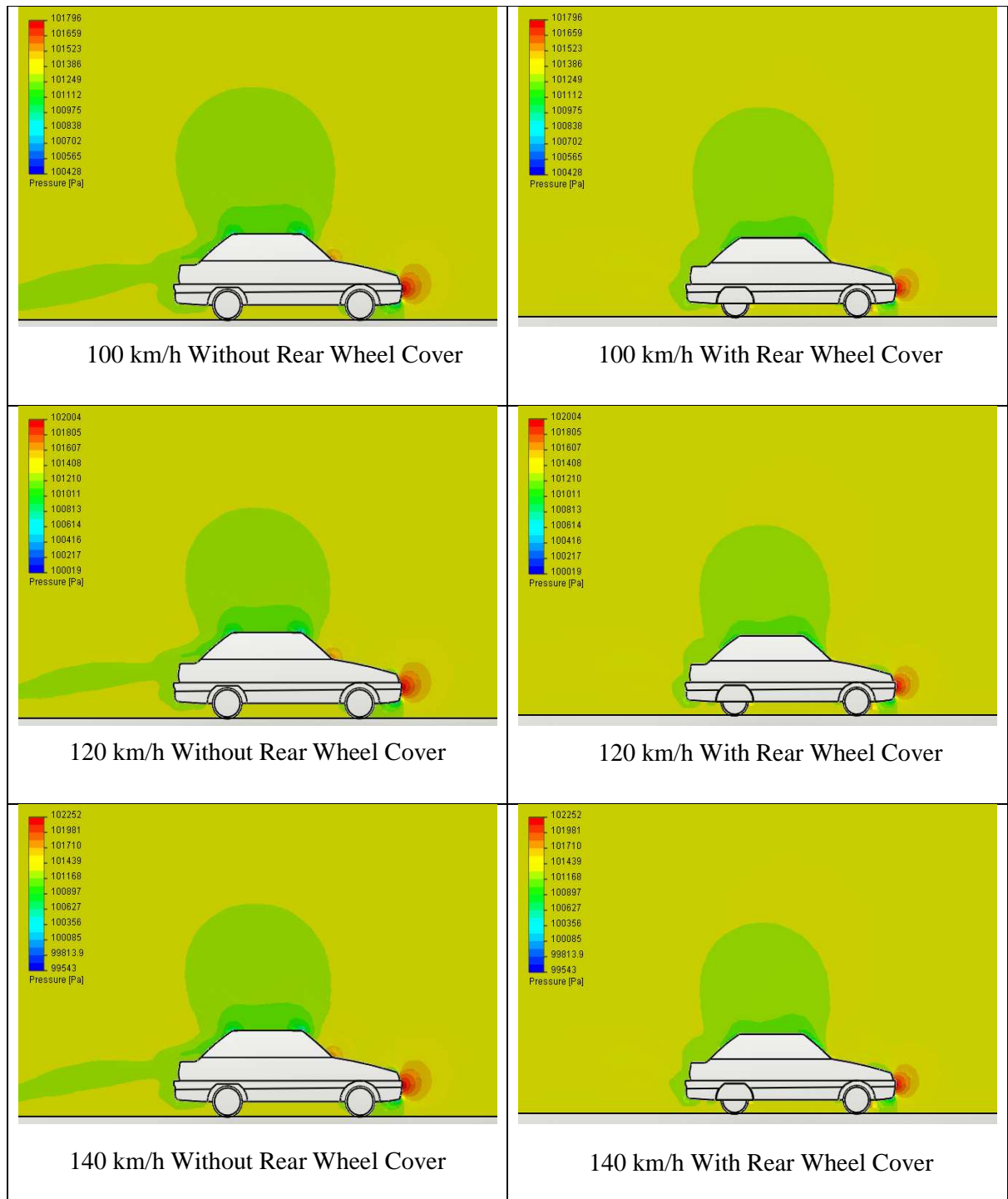
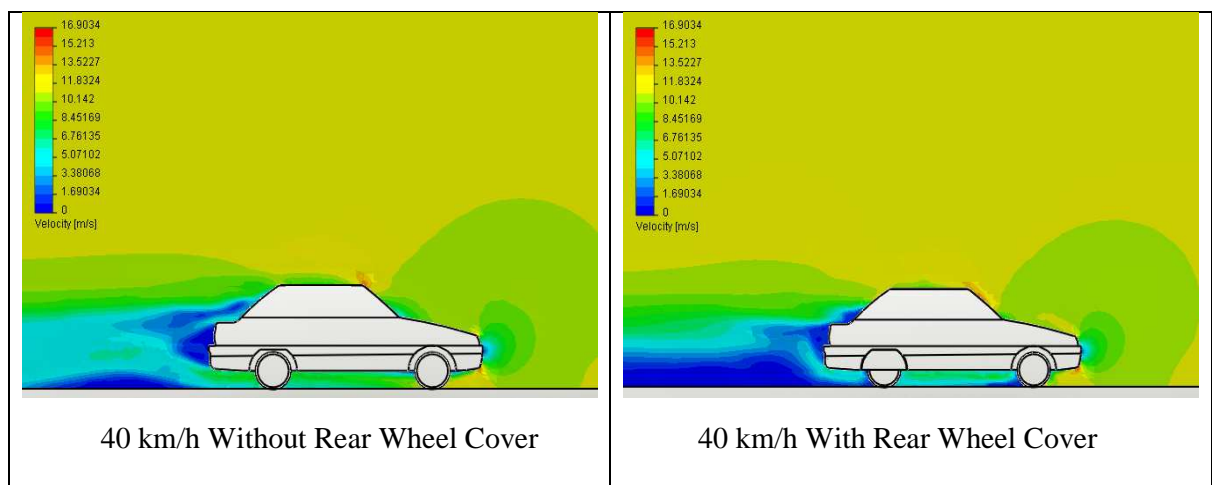


Figure 4.4: Comparison of pressure distribution between with and without rear wheel cover

The simulation result was taken on the symmetric plane. When the wheel cover device is installed on the model, the pressure at upper area of the rear boot will increase due to the increasing of velocity. This will make the model not easily slip or lift. The pressures at upper end profile of the model with wheel cover are higher compared with the model without rear wheel cover. The surrounding pressure of the model also higher compare with the model without rear wheel cover. As shown in figure, the pressure distributions are lower at the bottom of the underbody compared at the upper as the speeds are increase on model with rear wheel cover. Different pressure distribution at rear will influence for the model drag coefficient. Higher pressure also is located at the front bumper which the location where the stagnation point of the air flow to the model body. The spot between the front windscreen and front hood also contributed to the higher pressure. However there got a several location which is has the lowers pressure distribution at both the front and rear end of the underbody. From the scale, the higher value is 102252 Pa and the lowest is 99543 Pa. These lower pressure locations are important for the stability of the vehicle. The high pressure are refer as a positive pressure and the lower as a negative pressure. By comparing from these two conditions, the upper pressure distributions of rear wheel cover are higher than the model without rear wheel cover. These states the vehicle with rear wheel cover is better in term of drag coefficient.

4.6.2 Simulation of External Velocity Distribution

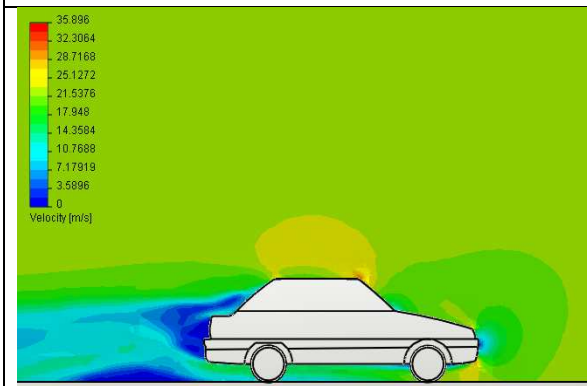




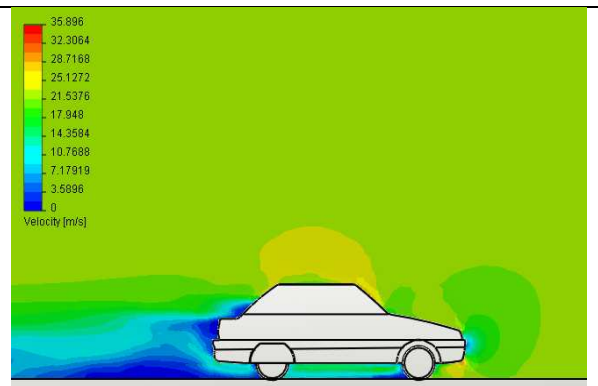
60 km/h Without Rear Wheel Cover



60 km/h With Rear Wheel Cover



80 km/h Without Rear Wheel Cover



80 km/h With Rear Wheel Cover



100 km/h Without Rear Wheel Cover



100 km/h With Rear Wheel Cover

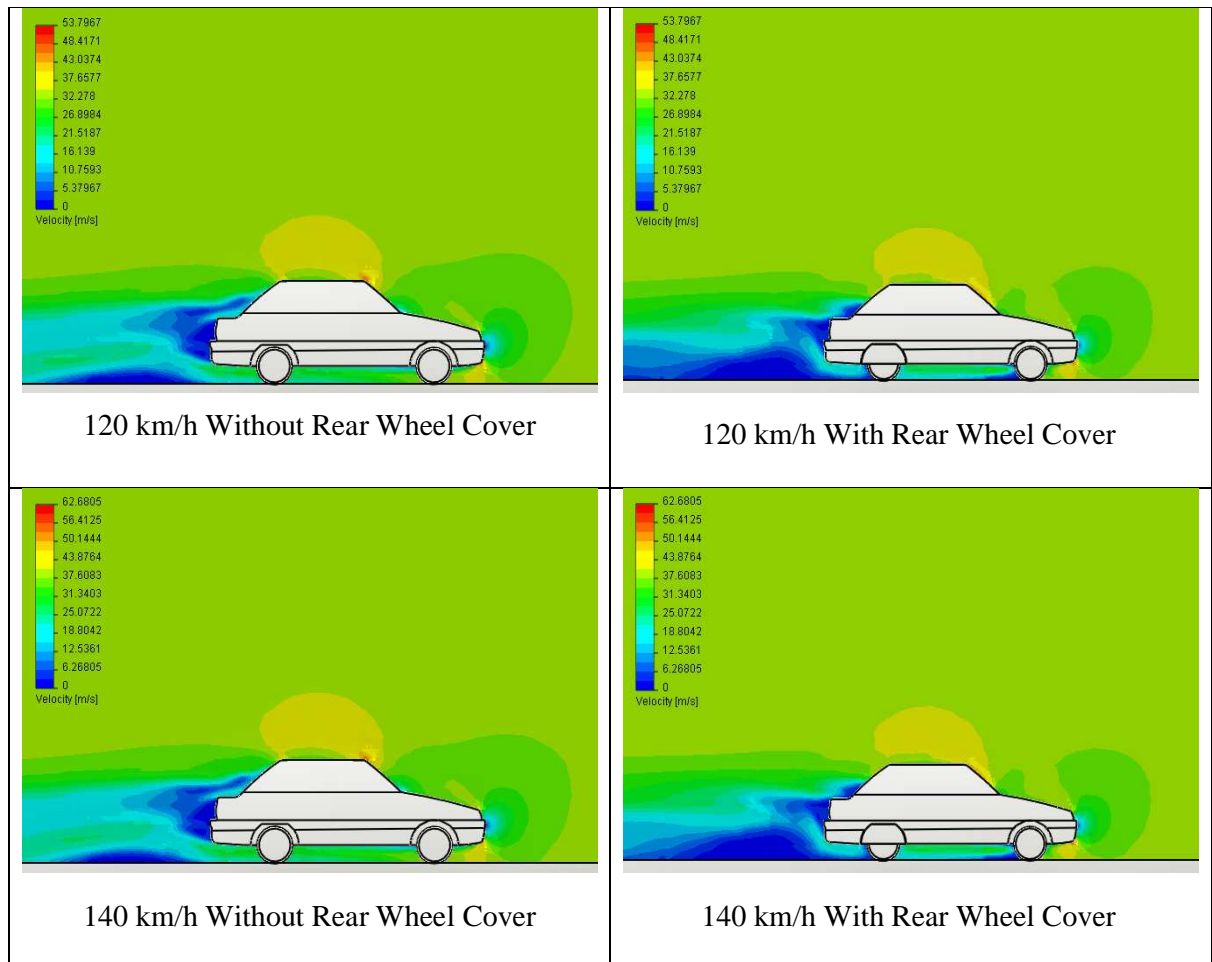


Figure 4.5: Comparison of velocity distribution between with and without rear wheel cover

The simulation result was taken on the symmetric plane. From the figure shown above, there are air flow stream that will change due to the increasing of the velocity. The flow also is difference between model with and without rear wheel cover. This is because of the flow separation at rear area that been helped by rear wheel cover. The flow stream will become slightly smaller that showed the flow separations at the rear model are became smaller too. But, the flow separation of the model with rear wheel cover device is smaller than model without rear wheel cover device. The wakes areas are produce when the vehicle is moving as show as the blue color regions. This region produces at the rear model area. These regions are called as reversed flow of the velocity. When the speed is increase, the rear flow separation will curved upward as the higher velocity. By installing the rear wheel cover device, the wake region will be

reducing. These reducing of wake region will improve the reduction of vehicle drag. So, the drag of the vehicle will reduce due to fuel consumption. At the speed of 140 km/h is clearly showed the reducing of the wake region at the rear area with the rear wheel cover. Low drag is required to attain high speed. Less of wake region will contribute the lower drag of moving body. These have shown at the model with rear wheel cover that is the wake region area is less than the model without rear wheel cover. These reducing of wake region happen because of the reducing flow separation at the back. From the scale, the higher value is 62.6805 m/s and the lowest is 0 m/s.

4.7 Discussion

As the pressure contribution at body, rear wheel cover will make a difference in performance at high speed. High speed will cause enough to reduce the drag force of the car when with rear wheel cover. The pressures at above of the vehicle body are lower than vehicle body with rear wheel cover. Also the pressures at underbody are higher than vehicle body with rear wheel cover. Rear wheel cover will make the body pressure lower than without rear wheel cover. These will make the car easily to move without drag and lift. Rear wheel cover will reduce the drag. The drag coefficient of the vehicle decreases from 0.3882 to 0.3773 by adding the rear wheel cover to the basic body and the P reduction effect for rear wheel cover were decrease from 10.1059 kW to 9.9610 kW. Pressure distribution from rear wheel cover will help vehicle to more stable when high speed and rear wheel cover will reduce the drag of vehicle especially in low velocity and fuel consumption.

From this simulation, there are several things can be carried out:-

- Any aerodynamic devices such as rear wheel cover, vortex generator, front and rear spoiler do have an effect on overall flow of the vehicles.
- Different velocity will give different result to the simulation because of the changing pressure and velocity distribution.

- The vehicles need to be modeled completely and choosing the fine value of meshing to get the better simulation data result.
- CFD gives a good approximation for the drag and drastically reduces cost for the development stage of vehicle body.

CHAPTER 5

CONCLUSION AND RECOMMENDATION

5.1 Conclusion

Drag force is the main issues for the road vehicles over the years. By reducing the drag force is the one of the solution to reduced fuel consumption, stability and handling particularly at high speed. It is well known that a large proportion of the drag is the result of pressure drag produced at the rear end of the vehicle and the understanding derived from the study of the wake structure is crucial in improving the road vehicle aerodynamic performance. For the road vehicles, it is basically three-dimensional bluff bodies in proximity to the ground.

By adding the aerodynamic devices like rear wheel cover, the result will decrease the pressure distribution at the rear of the vehicles. From the result, it is shown an improvement by adding the rear wheel cover as one of the aerodynamic devices.

This project is started by adding the rear wheel cover device on the HEV model by using CAD. The method to analyze this project is simulating the model using the CFD COSMOSFlow. From the analysis that had been finished, there is a different before and after the simulation is complete. This different can be seen clearly even by using an input data for both condition.

5.2 Recommendation

As for the future researches, the different length and different angle of rear wheel cover can be compared by simply attached to the same model to see the different of flow and also to determined is the design of the rear wheel cover also influent the characteristic of the flow. Some other recommendation can be carried out:-

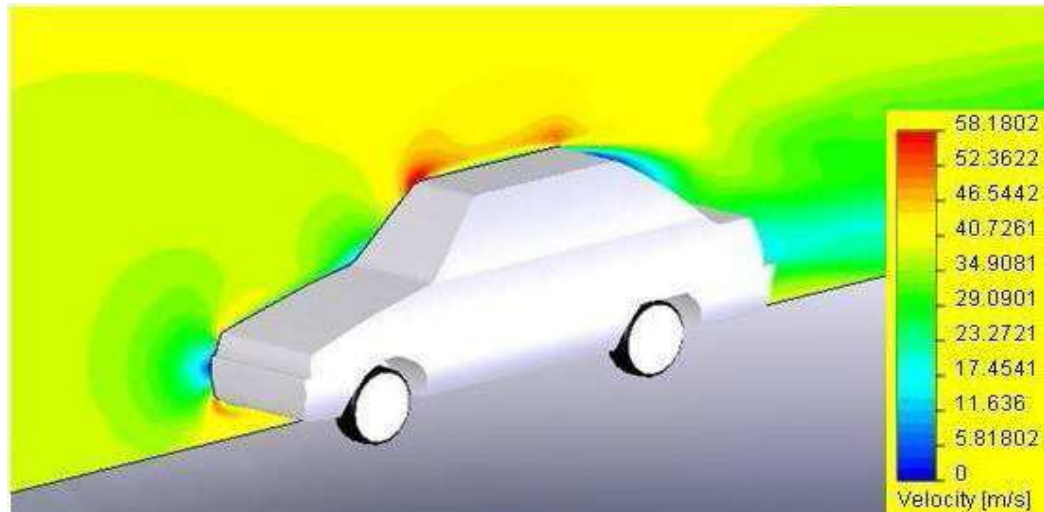
- Used the Computational Fluid Dynamic software (Fluent) to do the same analysis to see the different on data.
- Further analysis on other parts on the model such as side mirror, side skirt, vortex generator, and others beside the well-known aerodynamic devices.
- Determined the design of rear wheel cover also influent the characteristic of the flow.

REFERENCES

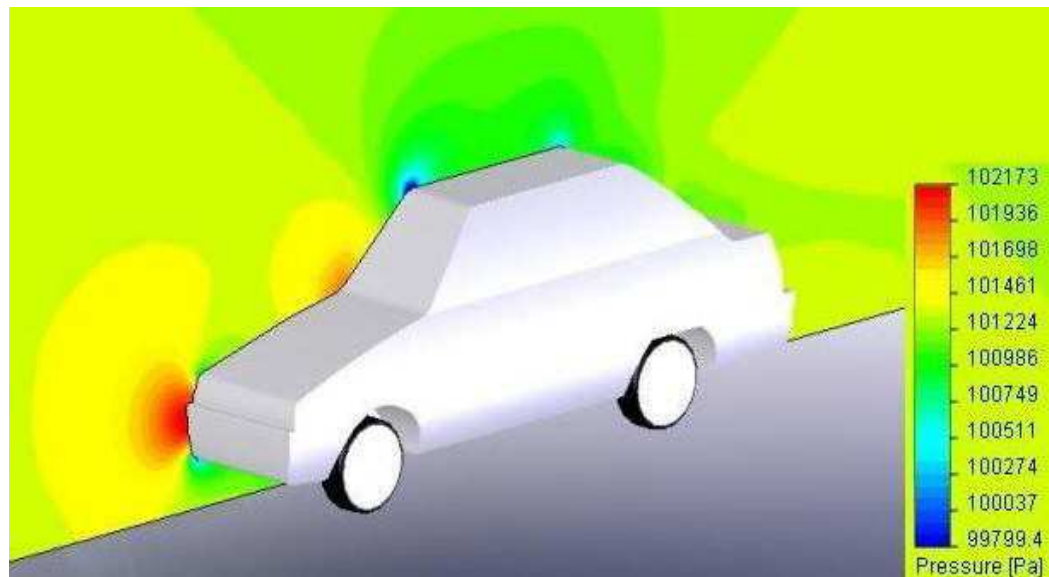
This guide is prepared based on the following references;

- [1] Thomas D. Gillespie. (2000). *Fundamentals of Vehicle Dynamics*. Pg 74-96
- [2] Yunus A. Cengal, John M.Cimbala. (2006). *Fundamentals of Fluid Mechanics*, 1st Edition In SI Units. Pg 562-600
- [3] Simon Watkins, Greg Oswald, *Journal of Wind Engineering and Industrial Aerodynamics 83 (1999)*, The Flow Field Of Automobile Add-ons-with particular reference to the vibration of external mirror. Pg 541-554.
- [4] Boris Epstein, Sergey Peigin, Shlomo Tsach, *Aerospace Science and Technology (2006)*, A New Efficient Technology of Aerodynamic Design Based on CFD Driven Optimization, pg 100-110
- [5] M.A.Leschziner, *Fluid Dynamics Research 38 (2006)*, *Modelling Turbulent Separated Flow in the Context of Aerodynamic Applications*, pg 174-210 59
- [6] Soo-Jin Jeong, Woo-Seung Kim, Sang-Jin Sung, *Medical Engineering & Physics 29 (2007)*, *Numerical Investigation On The Flow Characteristics And Aerodynamic Force of The Upper Airway of Patient With Obstructive Sleep Apnea Using CFD*, pg 637-651
- [7] S. Yongling (2003), *Numerical Simulation of the External Flow Field Around a Bluff Car*, Wu Guangqiang, Xieshuo Automotive Engineering Department Shanghai Tongji University Shanghai, China. pg 1-6

- [8] Michele Ferlauto, Roberto Marsilio, *Computer & Fluids* (2006), *A Viscous Inverse Method for Aerodynamic Design*, pg 304-325
- [9] Heisler. H. (2002). *Advanced Vehicle Technology*. Elsevier Butterworth Heinemann, Jordan Hill, Oxford. Pg 121-123
- [10] Tamás Rékert, Dr. Tamás Lajos. (2006). *The effect of wheels and wheelhouses on the aerodynamic forces acting on passenger cars*. Budapest University of Technology and Economics, Mechanical Faculty, Department of Fluid Mechanics, Hungary
- [11] Tamás Rékert, Dr. Tamás Lajos. (2006). *Numerical simulation of flow field past road vehicle wheel*. Hungary
- [12] John S. Paschkewit. (2006). *A computational study of tandem dual wheel aerodynamics and the effect of fenders and fairings on spray dispersion*. Oxford University Press
- [13] Emmanuelle Thivolle-Cazat, Patrick Gilliéron. (2006). *Flow analysis around a rotating wheel*. Lisbon, Portugal
- [14] Devarajan Ramasamy. (2005). *Development Of A Compressed Natural Gas (CNG) Mixer For A Two Stroke Internal Combustion Engine*. UTM
- [15] Johari Ismail. (2008). *Design and Analysis of Vortex Generator for a HEV Model*. UMP
- [16] Mohd Syazrin Sopnan. (2008). *Design And Analysis Rear Diffuser For Hev Model*. UMP

APPENDIX B**PLANE ANALYSIS PROFILE VISUALIZATION**

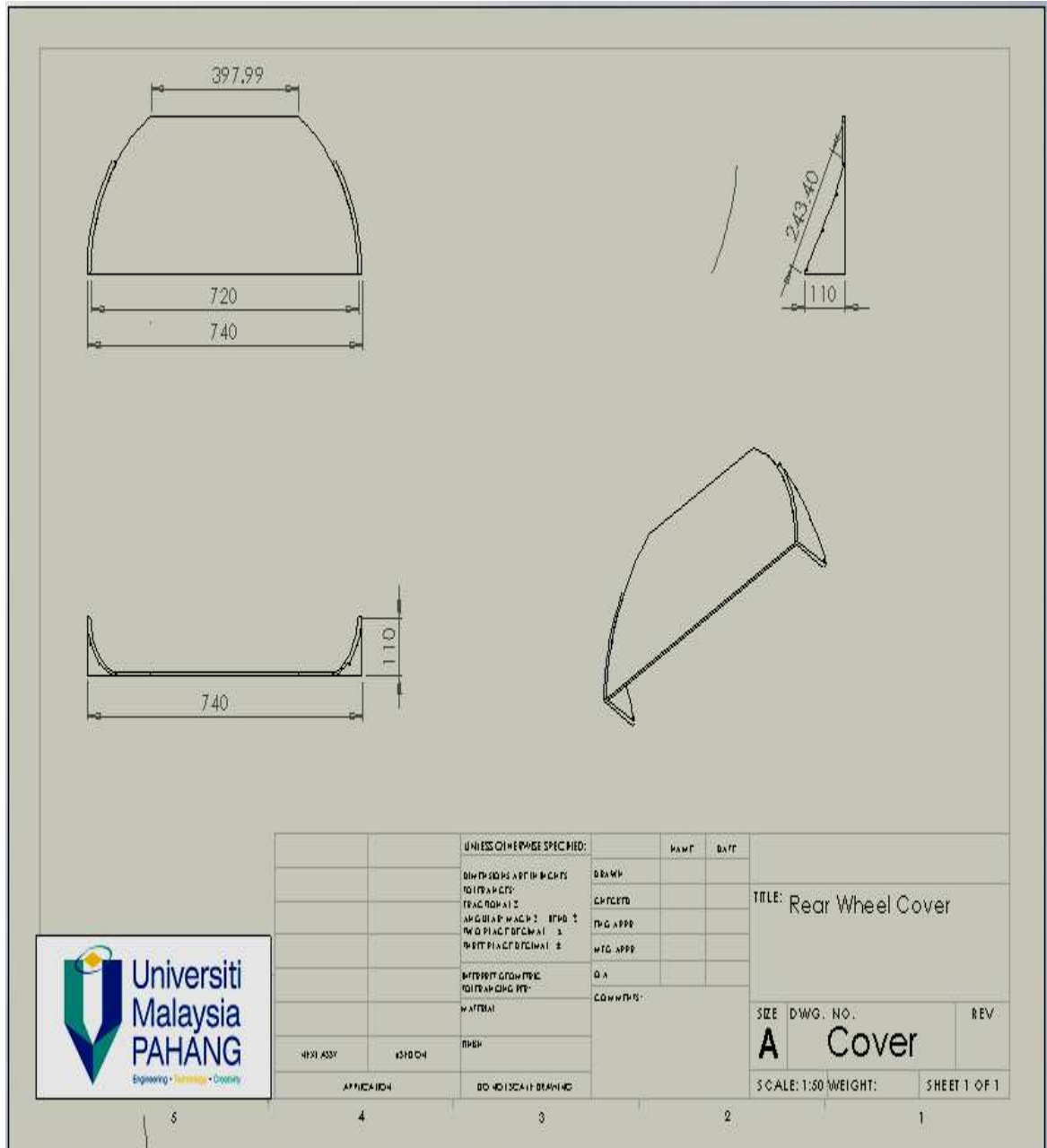
Symmetric plane at the center of the model body



Symmetric plane at the center of the model body

APPENDIX C

REAR WHEEL COVER MODEL



UNLESS OTHERWISE SPECIFIED:		DATE	
DIMENSIONS ARE IN MILLIMETERS	DRAWN		
TOLERANCES	CHECKED		
FRACTIONS	FIG APPR		
ANGULAR MEASUREMENTS	WTG APPR		
DECIMAL MEASUREMENTS	QA		
INTERPRET DIMENSIONS AND TOLERANCES TO THIS DRAWING PER:	COMMENTS		
MATERIAL			
FINISH			
4821 ASSY	4510 CH		
APPLICATION	DO NOT SCALE DRAWING		

TITLE: Rear Wheel Cover

SIZE	DWG. NO.	REV.
A	Cover	

SCALE: 1:50 WEIGHT: SHEET 1 OF 1

5 4 3 2 1

